NAVAL POSTGRADUATE SCHOOL

MONTEREY, CALIFORNIA

THESIS

STUDY OF LOAD TRANSFER AND FRACTURE ON COMPOSITE-TO-METAL-WIRE JOINTS

by

Mark F. Boseman

March 2009

Thesis Advisor:	Young W. Kwon
Second Reader:	Douglas C. Loup

Approved for public release; distribution is unlimited.

THIS PAGE INTENTIONALLY LEFT BLANK

REPORT DOCUMENTATION PAGE			Form Approved OMB No. 0704-0188
Public reporting burden for this collection of information is estimated to average 1 hour per response, including the time for reviewing instruction, searching existing data sources, gathering and maintaining the data needed, and completing and reviewing the collection of information. Send comments regarding this burden estimate or any other aspect of this collection of information, including suggestions for reducing this burden, to Washington headquarters Services, Directorate for Information Operations and Reports, 1215 Jefferson Davis Highway, Suite 1204, Arlington, VA 22202-4302, and to the Office of Management and Budget, Paperwork Reduction Project (0704-0188) Washington DC 20503.			
1. AGENCY USE ONLY ***(Leave blank)***	**2. REPORT DATE** March 2009	**3. REPORT TYPE AND DATES COVERED** Master's Thesis	
4. TITLE AND SUBTITLE Study of Load Transfer and Fracture on Composite-to-Metal-Wire Joints.		**5. FUNDING NUMBERS**	
6. AUTHOR(S) Mark F. Boseman			
7. PERFORMING ORGANIZATION NAME(S) AND ADDRESS(ES) Naval Postgraduate School Monterey, CA 93943-5000		**8. PERFORMING ORGANIZATION REPORT NUMBER**	
9. SPONSORING /MONITORING AGENCY NAME(S) AND ADDRESS(ES) N/A		**10. SPONSORING/MONITORING AGENCY REPORT NUMBER**	
11. SUPPLEMENTARY NOTES The views expressed in this thesis are those of the author and do not reflect the official policy or position of the Department of Defense or the U.S. Government.			
12a. DISTRIBUTION / AVAILABILITY STATEMENT Approved for public release; distribution is unlimited.		**12b. DISTRIBUTION CODE**	

13. ABSTRACT (maximum 200 words)

In order to connect a composite structure to a metallic structure, a hybrid composite/metal-wire laminate has been considered. Such a hybrid laminate raises a question of interface strength between the composite layer and metal-wire layer, and what kind of lay-up configuration would be the best. In order to answer the question, the following three joints were considered: butt joint, overlap joint, and modified-wire-end-shape joint. The goal of this research was to numerically determine which joint would be the strongest based on its components of fracture toughness under various loading conditions such as tension, shear and bending. A defect was included between and parallel to the interfaces to simulate a crack in the critical regions of the models. The crack growth, due to interlaminar tension and/or sliding, is analyzed using the crack closure technique. Finite element formulations in this research are carried out by using ANSYS finite element software.

14. SUBJECT TERMS butt joint, overlap joint, modified-wire-end-shape joint, finite element method, energy release rate, virtual crack closure method, fracture toughness, ansys			**15. NUMBER OF PAGES** 60
			16. PRICE CODE
17. SECURITY CLASSIFICATION OF REPORT Unclassified	**18. SECURITY CLASSIFICATION OF THIS PAGE** Unclassified	**19. SECURITY CLASSIFICATION OF ABSTRACT** Unclassified	**20. LIMITATION OF ABSTRACT** UU

NSN 7540-01-280-5500 Standard Form 298 (Rev. 2-89)
Prescribed by ANSI Std. 239-18

THIS PAGE INTENTIONALLY LEFT BLANK

Approved for public release; distribution is unlimited.

STUDY OF LOAD TRANSFER AND FRACTURE ON COMPOSITE-TO-METAL-WIRE JOINTS

Mark F. Boseman
Lieutenant, United States Navy
B.S., Saint Louis University, 1998

Submitted in partial fulfillment of the
requirements for the degree of

MASTER OF SCIENCE IN MECHANICAL ENGINEERING

from the

NAVAL POSTGRADUATE SCHOOL
March 2009

Author: Mark F. Boseman

Approved by: Young W. Kwon
Thesis Advisor

Douglas C. Loup
Second Reader

Knox Millsaps
Chairman, Department of Mechanical and Astronautical Engineering

THIS PAGE INTENTIONALLY LEFT BLANK

ABSTRACT

In order to connect a composite structure to a metallic structure, a hybrid composite/metal-wire laminate has been considered. Such a hybrid laminate raises a question of interface strength between the composite layer and metal-wire layer, and what kind of lay-up configuration would be best. In order to answer the question, the following three joints were considered: butt joint, overlap joint, and modified-wire-end-shape joint. The goal of this research was to numerically determine which joint would be the strongest based on its components of fracture toughness under various loading conditions such as tension, shear and bending. A defect was included between and parallel to the interfaces to simulate a crack in the critical regions of the models. The crack growth, due to interlaminar tension and/or sliding, is analyzed using the crack closure technique. Finite element formulations in this research are carried out by using ANSYS finite element software.

THIS PAGE INTENTIONALLY LEFT BLANK

TABLE OF CONTENTS

THIS PAGE INTENTIONALLY LEFT BLANK

LIST OF FIGURES

LIST OF TABLES

ACKNOWLEDGMENTS

Professor Young Kwon, for all the support, guidance and patience during the course of my research and graduate studies.

Most of all, to my Maker.

THIS PAGE INTENTIONALLY LEFT BLANK

I. INTRODUCTION

A. BACKGROUND

Composite materials are increasingly being used in aerospace, underwater, and automotive structures. The application of composite materials to engineering components has spurred a major effort to analyze structural components made from them. Composite materials provide unique advantages over their metallic counterpart, but they also present complex and challenging problems to analysts and designers [1].

Composite materials are those that consist of two or more constituent materials that together produce desirable properties for a given application. Fiber-reinforced composite materials are the most commonly used modern composite material that consist of high strength and high modulus fibers in a binding matrix material. In these composites, fibers are the principal load-carrying members, and the matrix material keeps the fibers together, acts as a load-transfer medium between fibers, and protects the fibers from being exposed to the environment [1].

Fiber-reinforced composite materials for structural applications are often made in the form of a thin layer, called lamina. Structural elements are then formed by stacking the layers to desired thickness and properties. Fiber orientation in each lamina and stacking sequence of the layer can be chosen to achieve desired strength and stiffness for a specific application [1].

The most common failure mode for composite structures is delamination. The remote loadings applied to composites components are typically resolved into interlaminar tension and shear stresses at discontinuities, which create mixed-mode I, II, III delaminations. To characterize the onset and growth of these delaminations the use of fracture mechanics has become common practice over the past two decades. The total strain energy release rate G_T, the mode I component due to interlaminar tension, G_I, the mode II components due to interlaminar sliding shear, G_{II}, and the mode III component, G_{III}, due to interlaminar scissoring shear need to be calculated. In order to predict the delamination onset or growth for two-dimensional problems, these G components are

compared to interlaminar fracture toughness properties measured over a range from pure mode I loading to pure mode II loading [2]. Failure is expected when, for a given energy release rate G_i exceeds the interlaminar fracture toughness G_{ic}, where i is either mode I, mode II or mixed mode. The virtual crack closure technique (VCCT) is widely used for computing energy release rates based on results from continuum (2D) and solid (3D) finite element analyses to supply mode separation required when using the mixed-mode fracture criterion [2].

B. SIMPLEST FORM OF JOINTS

In connecting separate sections of laminate structures, several configurations were made to improve the effectiveness of joints for certain design criteria. Some of the joint designs commonly used in manufacturing are the symmetric step/butted joint and step overlap joint as shown in Figure 1.

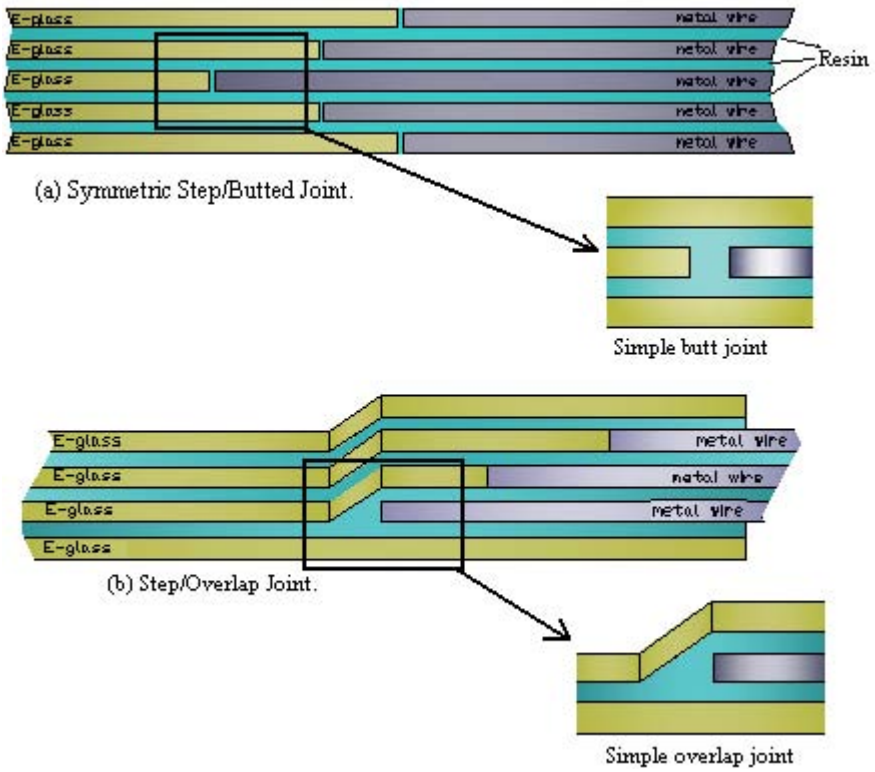

Figure 1. Symmetric Step/Butted Joint and Step Overlap Joint.

To make a good comparison on how the joint geometry affects the fracture toughness of these joints, the analysis will be performed on the building blocks of these joint designs, such as its simplest form shown in Figure 1. An analysis of modifying the wire end shape, in the case of the butt joint, will also be made to determine how it affects the fracture toughness.

THIS PAGE INTENTIONALLY LEFT BLANK

II. FINITE ELEMENT FORMULATION

A. MODEL GEOMETRY

The composite materials considered in for the models are the standard 24 oz. E-glass woven roving, 3SX unidirectional plies, and Vinyl-ester resin. The constituent model of the joint was created using fiber thicknesses of 1.27 mm (0.050 in) for both glass and steel fibers [6] and a resin layer thickness of 0.05mm (0.002 in) between fibers. The glass fibers, steel fibers, and resin were each modeled as isotropic using individual constituent properties given in Table 1 through Table 3 from reference [6].

Table 1. Properties of Steel Fiber

Property		Value	Units
Modulus	E	207	GPa
Poisson's Ratio	ν	0.3	
Shear Modulus	G	79.3	GPa

Table 2. Properties of E-Glass Fiber

Property		Value	Units
Modulus	E	72.4	GPa
Poisson's Ratio	ν	0.22	
Shear Modulus	G	30.0	GPa

Table 3. Properties of Dow Derakane 510A Vinyl-ester Resin

Property		Value	Units
Modulus	E	3.50	GPa
Poisson's Ratio	ν	0.32	
Shear Modulus	G	1.33	GPa

For the different types of joints, shown in Figure 2, in the case of the butt joint and the modified-wire-end-shape joint the distance d was assume to be 0.05 mm (.002 in). For the overlap joint the distance d was assumed to be 1.32 mm (0.052 in), creating an overlap angle of 45 degrees.

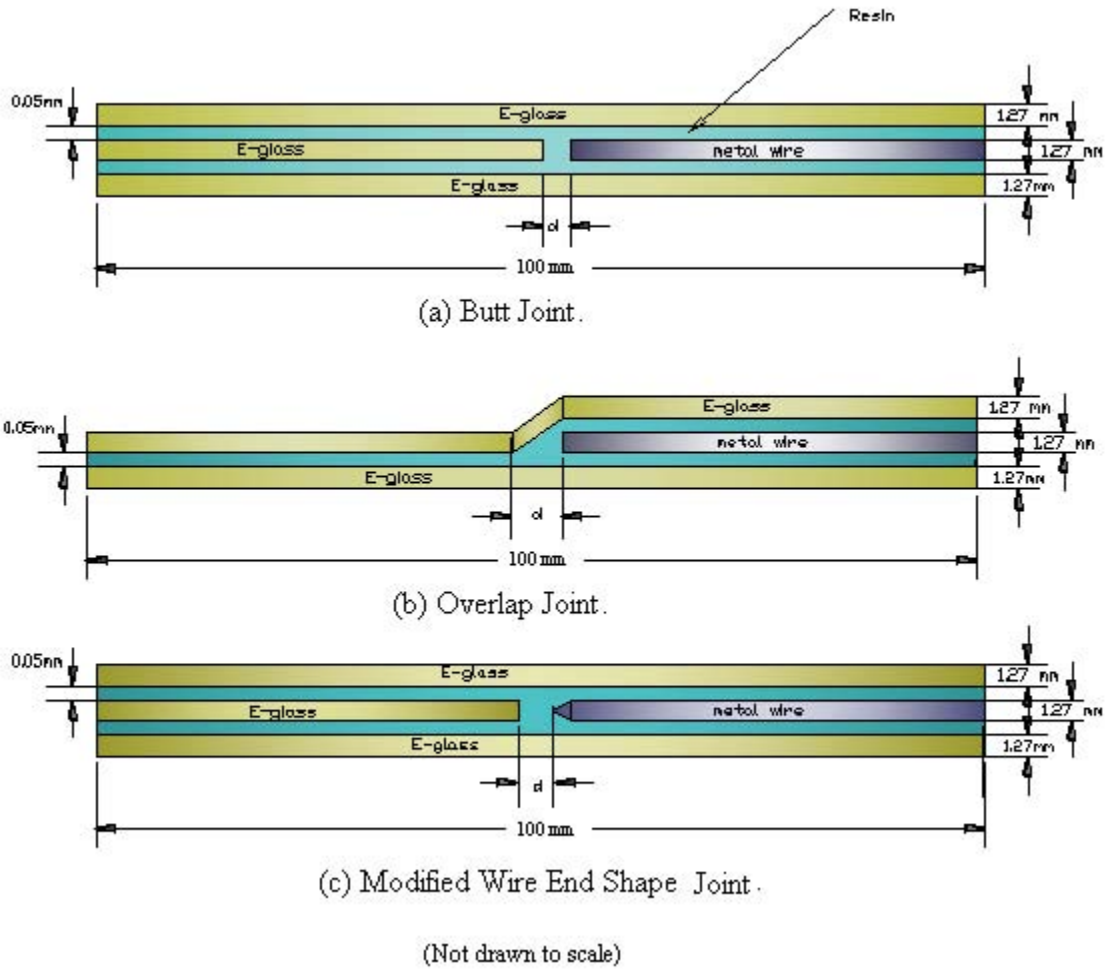

Figure 2. Model Dimensions.

B. LOADING AND CRITICAL CRACK LOCATIONS

Different load configurations, as shown in Figure 3, were applied to the three types of joint models. The left ends of the specimens were structurally fixed while right ends were subjected to the following loads: tension (uniform displacement load normalized to 1MPa), shear (1 KN) and bending (1KN-m). It has been observed in many experimental testing that the failure due to delamination initiates and propagates through the resin. Since the resin strength is very low compared to the e-glass and metal-wire, in this case it acts like an adhesive layer between the fibers. Under a certain load when

localized strain in the resin causes the fracture toughness to exceed the critical fracture toughness, the crack will propagate; thus, particular attention was given the strain of the resin in determining the critical locations.

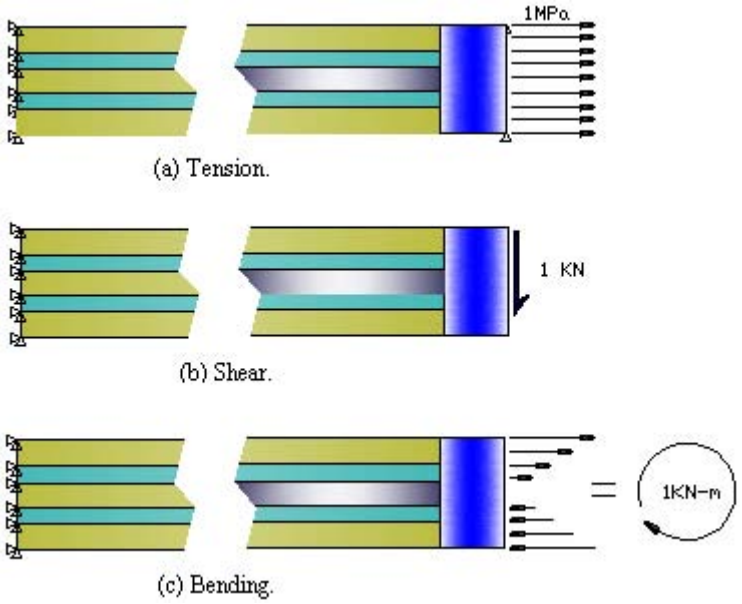

Figure 3. Load Configurations.

In finding the energy release rate components, the critical locations where delamination is most likely to occur was first determined. This was done by determining the locations that had the highest total mechanical strain in the resin layer of the model without defects. Then, at the region where the resin was subjected to high strain, crack inclusions in the model were placed inside the resin, metal-wire/resin interface and e-glass/resin interface.

C. CRACK GEOMETRY

The crack closure method requires an assumed initial flaw to be built into the finite element model. The length of this flaw is typically not known, so often the flaw is assumed to be less than what is detectable by inspection. “Undetectable” lengths commonly vary from 0.127 mm (0.005 inch) to 0.254 mm (0.01 inch) [4]. For this research, the assumed length was set at 0.254 mm (0.01 inch) and the element crack

extension Δa was set to 0.0127 mm (5% of crack length) for all models. Figure 4, in the case of the butt joint, shows the crack dimensions included in the model. The split interface, crack length of 0.254 mm plus the crack extension Δa, represents a discontinuity by a line of nodes, as shown in Figure 4. The crack tips, on both ends of the crack, each have a single node that connects the upper and lower elements. Nodes at the top surface and bottom surface of the split interface have identical coordinates, however, are not connected with each other. This discontinuity allows the elements connected to the top surface of the crack deform independently from those connected to the bottom surface. The tip on the right side was extended to serve as the element crack extension Δa.

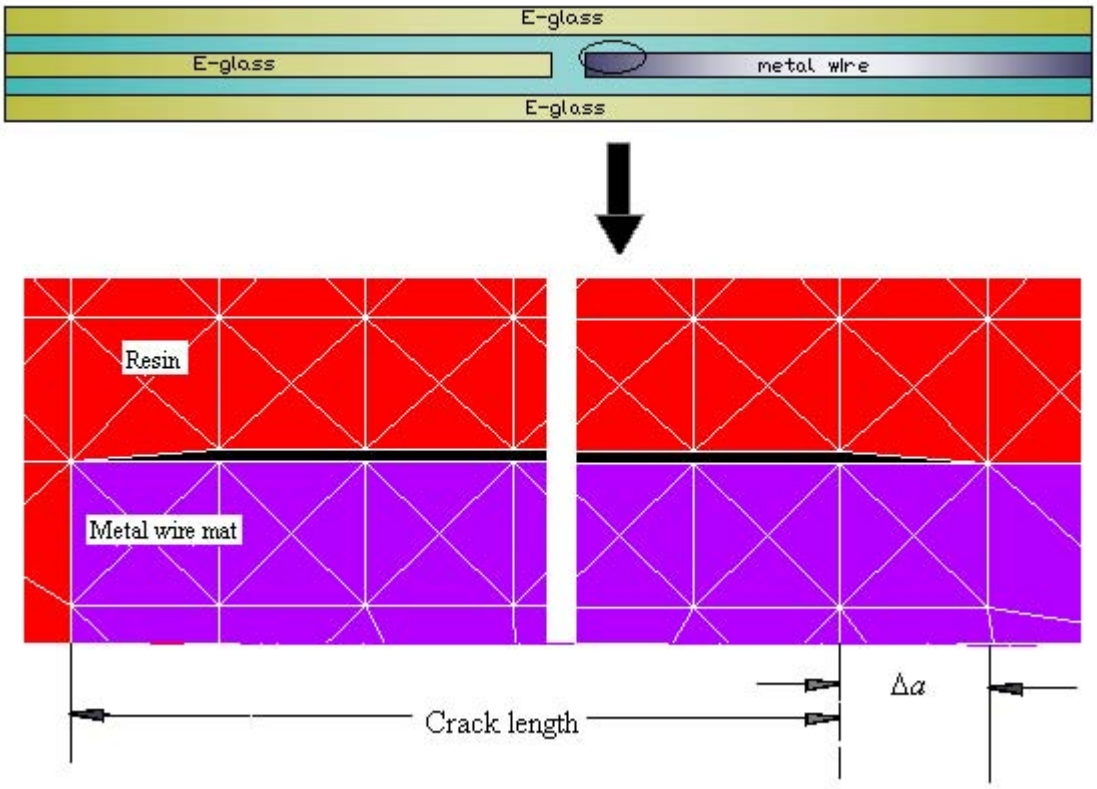

Figure 4. Crack Geometry.

D. VIRTUAL CRACK CLOSURE TECHNIQUE (VCCT)

An overview of the virtual crack closure technique (VCCT) and the modified VCCT, as published in reference [2], are presented in this research to show the different methods used in determining the components of fracture toughness. In this research the one step approach, modified VCCT, was employed using the two-dimensional, six-noded elements.

1. Virtual Crack Closure Technique

In this two step method, also called *crack closure technique*, the crack in the model is physically extended, or closed, during two complete finite element analyses as shown in Figure 5, where four-noded quadrilateral elements are used. The crack closure method is based on Irwin's crack closure integral. The method is based the assumption that the energy released when the crack is extended by Δa from a (Figure 5a) to $a + \Delta a$ (Figure 5b) is identical to the energy required to close the crack between location ℓ and i (Figure 5a) [2].

The modes I and II energy release rates, G_I and G_{II}, are calculated using the following equations:

$$G_I = \frac{1}{2\Delta a} Z_\ell \left[w_\ell - w_{l^*} \right] \qquad (1)$$

$$G_{II} = \frac{1}{2\Delta a} X_\ell \left[u_\ell - u_{\ell^*} \right] \qquad (2)$$

As shown in Figure 5, the forces are obtained from the first finite element analysis where the crack is closed. The displacements are obtained from the second finite element analysis where the crack is extended to one full element length.

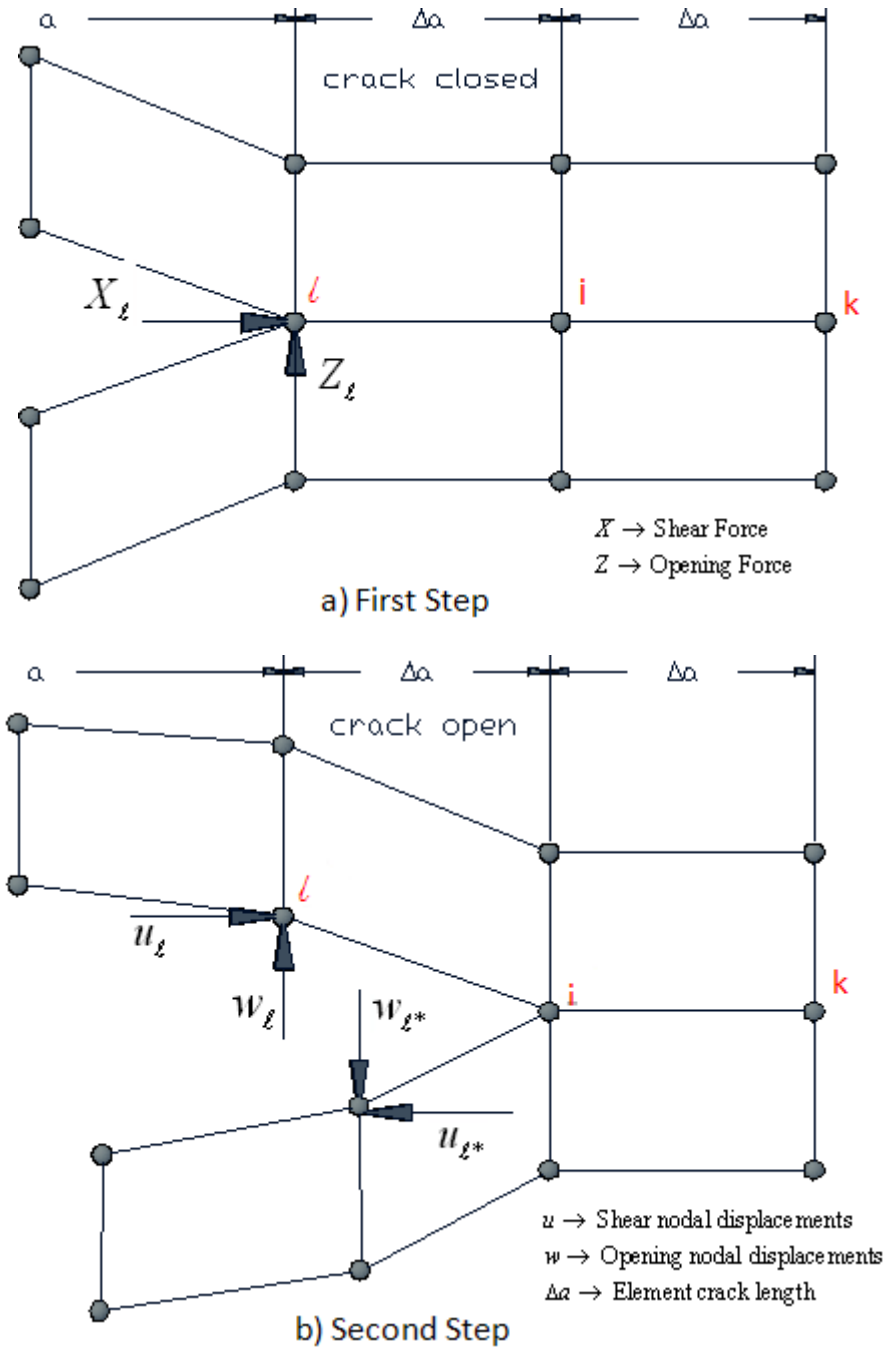

Figure 5. Two Step Virtual Crack Closure Technique for Four-Noded Element.

2. Modified Virtual Crack Closure Technique

The modified VCCT is based on the same assumptions as the two-step VCCT. Additionally, however, it is assumed that a crack extension of Δa from $a+\Delta a$ (node i) to $a+2\Delta a$ (node k) does not significantly alter the state at the crack tip (Figure 6). Therefore the displacements behind the crack tip at node i are approximately equal to the displacements behind the original crack tip at node ℓ. Reference [2] outlines the details for a crack modeled with two-dimensional, four-noded and eight-noded elements. Figure 6 show the modified VCCT using the two-dimensional, six-noded elements.

The modes I and II energy release rates, G_I and G_{II}, are calculated using the following equations:

$$G_I = \frac{1}{2\Delta a}\left[Z_i \left(w_\ell - w_{\ell *} \right) + Z_j \left(w_m - w_{m*} \right) \right] \qquad (1)$$

$$G_{II} = \frac{1}{2\Delta a}\left[X_i \left(u_\ell - u_{l*} \right) + X_j \left(u_m - u_{m*} \right) \right] \qquad (2)$$

In addition to the forces X_i and Z_i at the crack tip, the forces X_j and Z_j at the mid-side node in front of the crack are required. Also, in addition to the relative sliding and opening at nodal points ℓ and $\ell *$, the relative displacements at nodal points m and $m*$ are required.

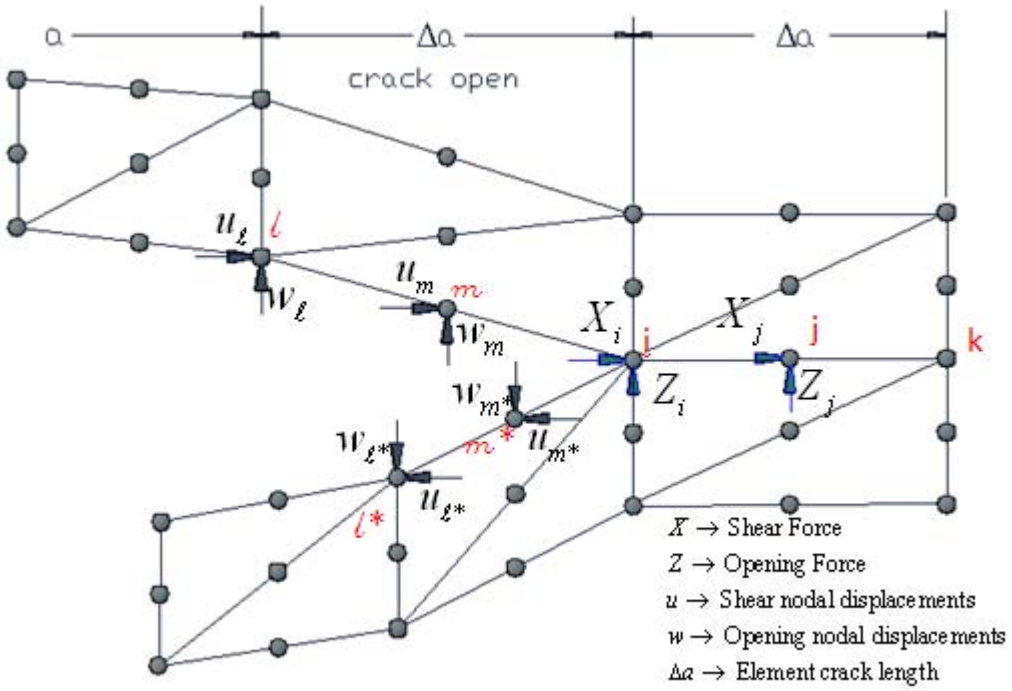

Figure 6. Virtual Crack Closure Technique for Six-Noded Element (One step).

III. ANALYSIS AND RESULTS FOR LOADING IN TENSION

A. RESULTS AND DISCUSSION

1. Critical Locations

The resulting effective mechanical strain plots of the models, without defects, under tension, are shown in Figure 7 through 9. The regions of high strain for the butt joint are located around the left edge corners of the metal-wire mat. Since the upper and lower strain fields are symmetrical about its centerline, the upper half (Figure 7) of the model was considered for the analysis. For the overlap joint, three critical crack locations were considered since the resulting plot (Figure 8) shows three regions of high strain. In the case of the modified-wire-end-shape joint, the regions of high strain are located at the apex and corners of the wire tip (Figure 9). Similar to the butt joint, the upper half of the model was considered for the analysis since the strain fields are also symmetrical about its centerline.

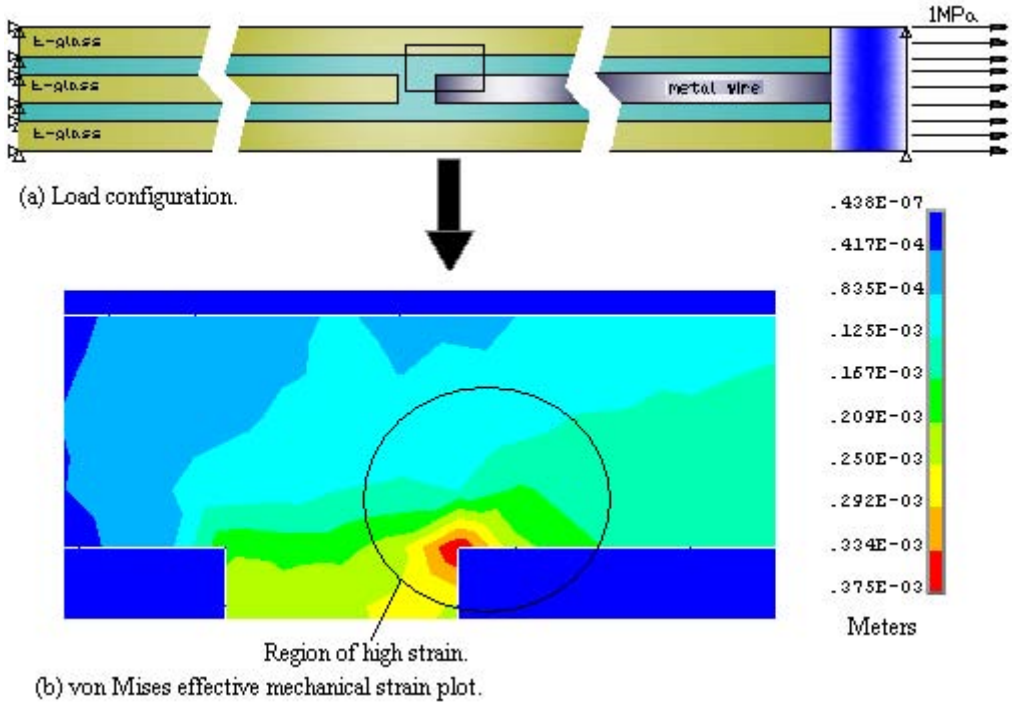

Figure 7. Butt Joint Critical Location.

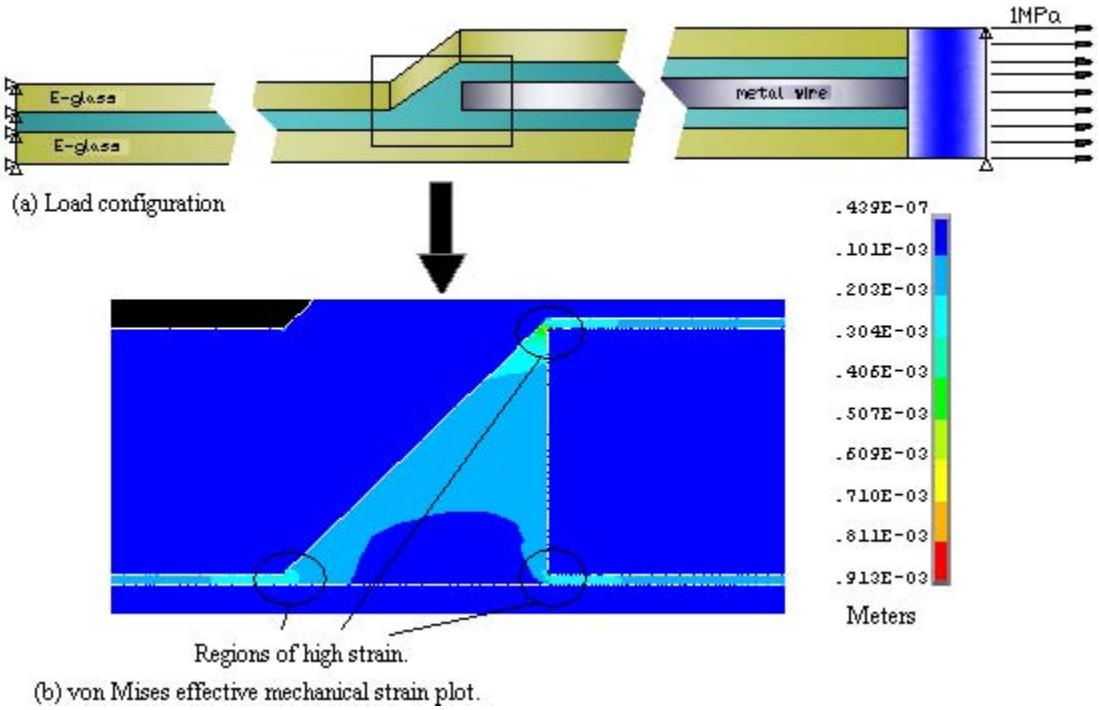

Figure 8. Overlap Joint Critical Location.

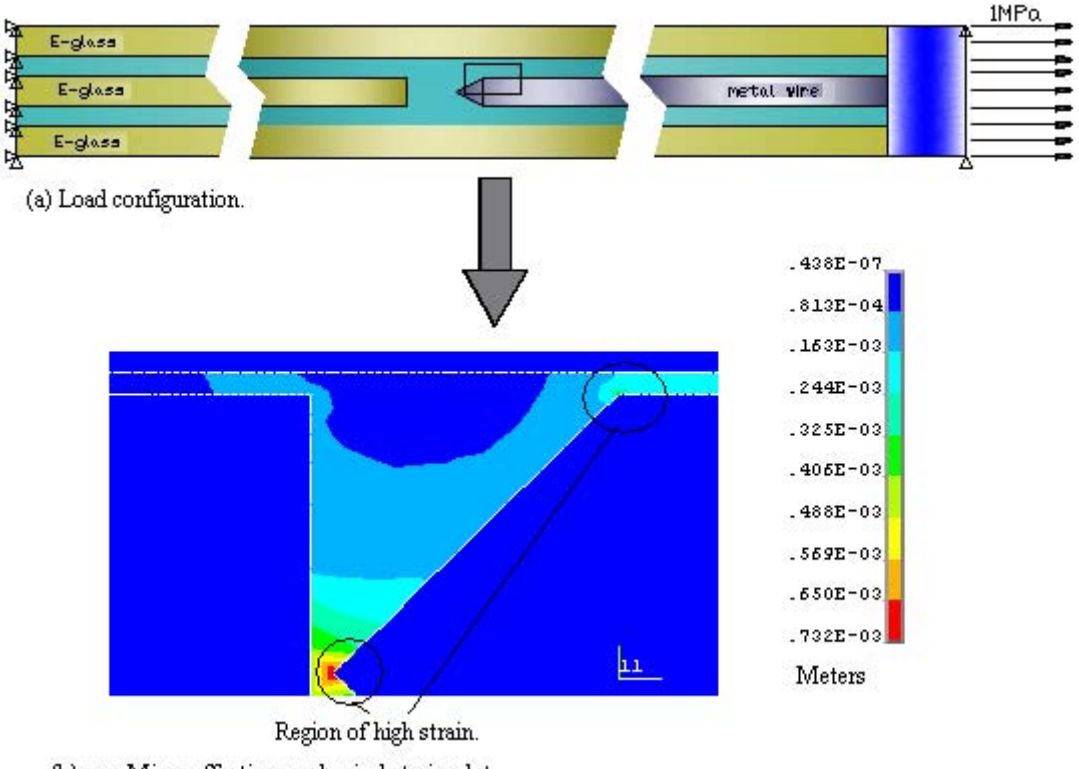

Figure 9. Modified-Wire-End-Shape Joint Critical Location.

In this load case, the outer composite layers carry most of the load at the joint due to the discontinuity of the middle layers. Because of the discontinuity, the load transfer from the left to middle composite layer to the right middle metal-layer occurs though shear stress between the middle metal layers and the surrounding resin layer. In addition, the resin between the two discontinuous composite and metal layers is under tensile stress. Thus, the onset of crack growth in the resin may occur due to interlaminar shear stress between the middle metal layer and the outer composite layers as well as due to tensile stress between the two middle layer tips. Thus, particular attention was given separately to the resin cracks between the middle and outer layers, and between the two middle layer tips (Figure 10).

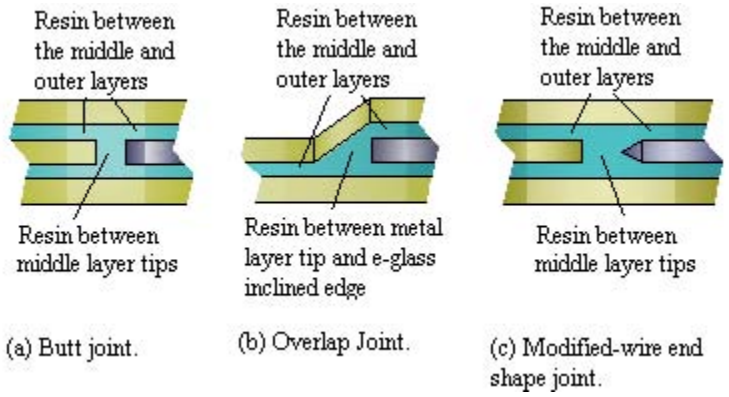

Figure 10. Description of Resin Sections.

2. Energy Release Rate Results

a. Butt Joint

In Location 1 through 3 in Figure 11, it was observed that the forces acting on the crack are closing in nature. This means that the mode I energy release rate component is non-existent and the energy release rate is purely mode II for resin cracks located between the fibers. The energy release rate results shows that the crack inside the resin, Location 2 in Figure 11, is the most critical case.

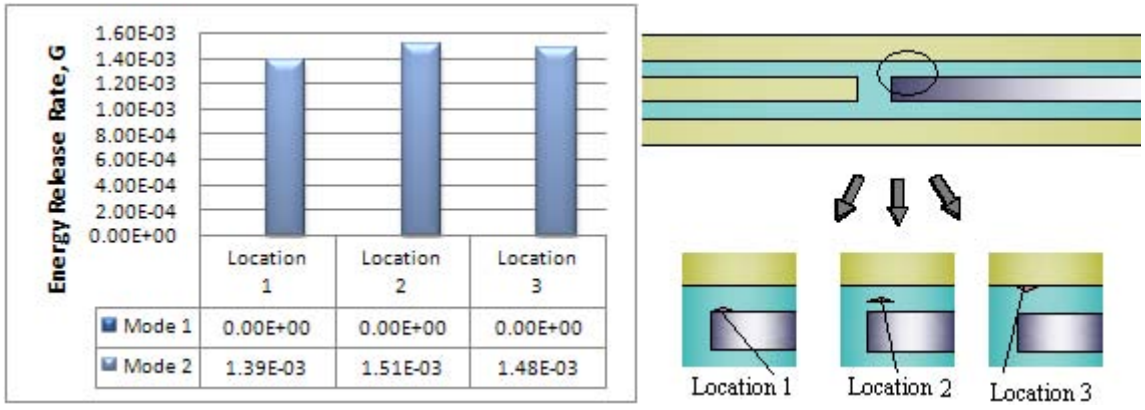

Figure 11. Butt Joint: Energy Release Rate of Resin Cracks between the Fibers.

In Location 4 through 6 in Figure 12, it was observed that the forces acting on the crack are tensile in nature and the forces due shearing are negligible. Thus, the mode I energy release rate component characterizes the failure of cracks existing between the fiber tips. Figure 12 shows Location 5, which is the crack located inside the resin, is the most critical case.

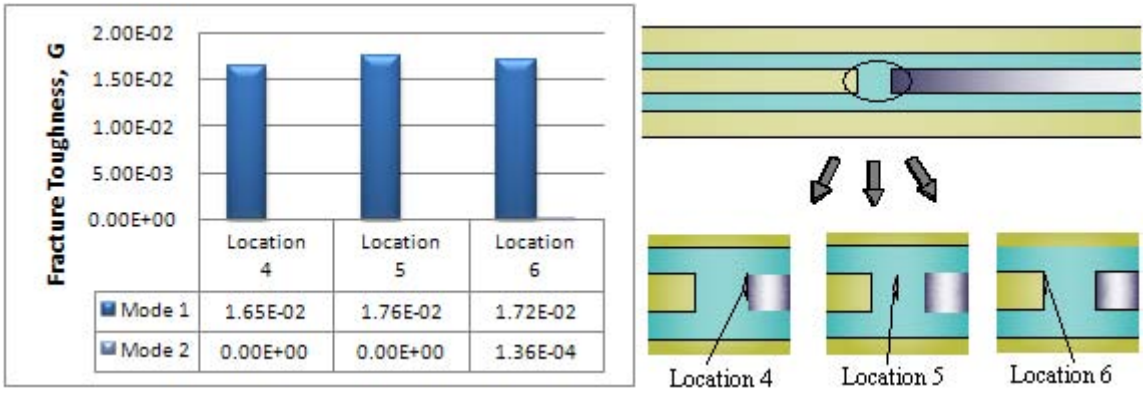

Figure 12. Butt Joint: Energy Release Rate of Resin Cracks between the Fibers Tips.

b. Overlap Joint

In Location 1 through 9 in Figure 13, it was observed that the interlaminar forces acting on the crack are sliding in nature. This means that the mode II characterizes the delamination failure for resin cracks located between the fibers. The energy release rate results shows that the crack inside the resin, Location 8 in Figure 13, is the most critical case.

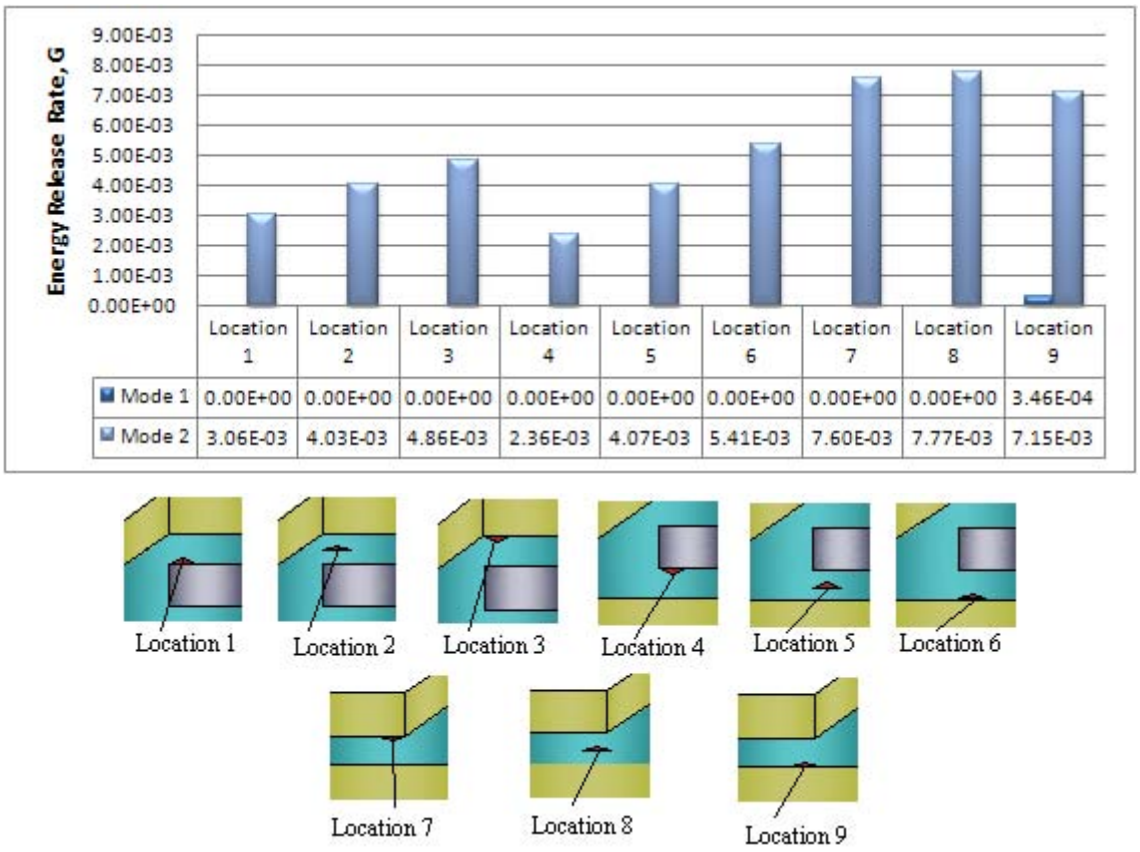

Figure 13. Overlap Joint: Energy Release Rate of Resin Cracks between the Fibers.

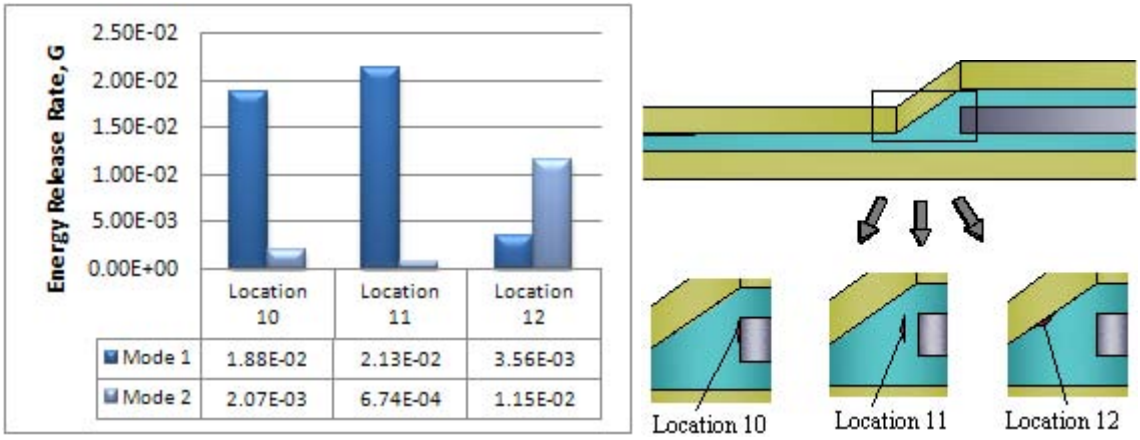

Figure 14. Overlap Joint: Energy Release Rate of Resin Cracks between Fibers Tips.

In Location 10 and 11 in Figure 14, it was observed that the forces acting on the crack are dominantly tensile in nature; therefore mode I component is the more significant component of failure for the cracks located between the fiber tips. The results

for the crack in Location 12 show that the mode I and II components are both significant, however, since mode I failure has usually a lower threshold than mode II, mode I results were considered as the determining factor for the most critical location. Thus, Location 11 was considered the most critical case.

c. Modified-Wire-End-Shape Joint

In Location 1 through 3 in Figure 15, similar to the butt joint, the mode II component characterizes the delamination failure for resin cracks located between the fibers. The energy release rate results shows that the crack along the e-glass interface, Location 3 in Figure 15, is the most critical case.

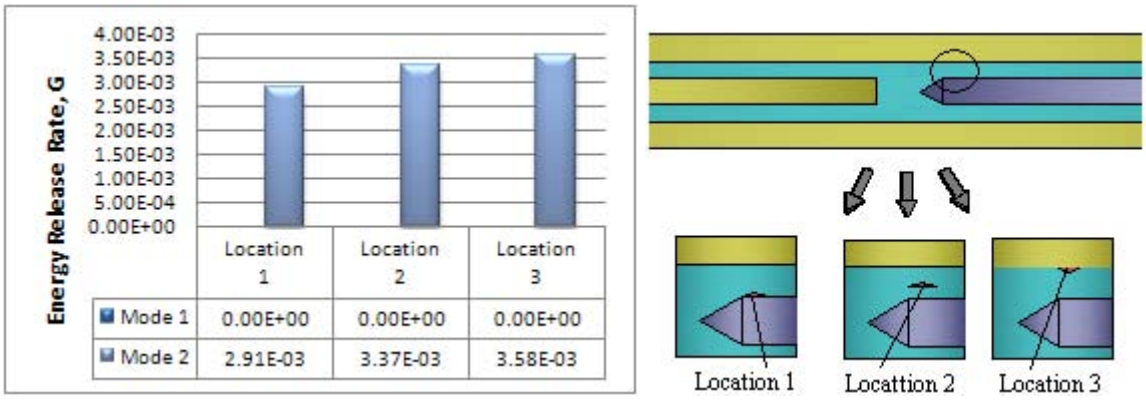

Figure 15. Modified-Wire-End-Shape Joint: Energy Release Rate of Resin Cracks between the Fibers.

In Location 4 through 6 in Figure 16, the forces acting on the crack are dominantly tensile in nature; thus, the mode I energy release rate component characterizes the delamination failure of cracks existing between the fiber tips. Location 6, which is the resin crack located along the e-glass interface, is the most critical case.

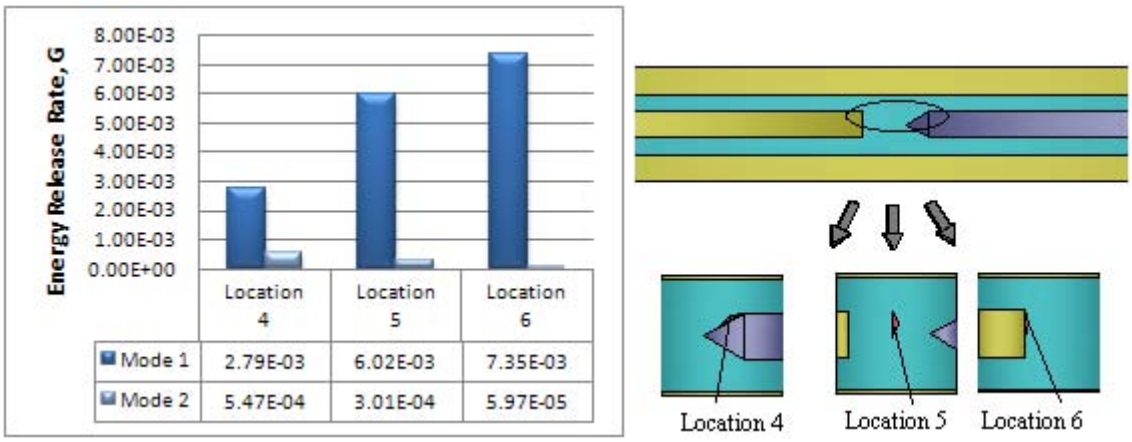

Figure 16. Modified-Wire-End-Shape Joint: Energy Release Rate of Resin Cracks between the Fiber Tips.

B. SUMMARY

Figure 17 and 18 shows the comparison of the energy release rate for each joint design. It was observed that the overlap joint has the highest energy release rate results for resin cracks between the fibers and in between the two fiber tips. For resin cracks between the fibers, the butt joint gave lower energy release rate results than the modified-wire-end-shape joint. However, for the resin cracks between the fiber tips, the modified-wire-end shape joint gave lower results. In the crack locations investigated, the most critical case for the butt joint and overlap joint are the cracks inside the resin. For the modified-wire-end-shape joint, cracks along the e-glass interface was the most critical case.

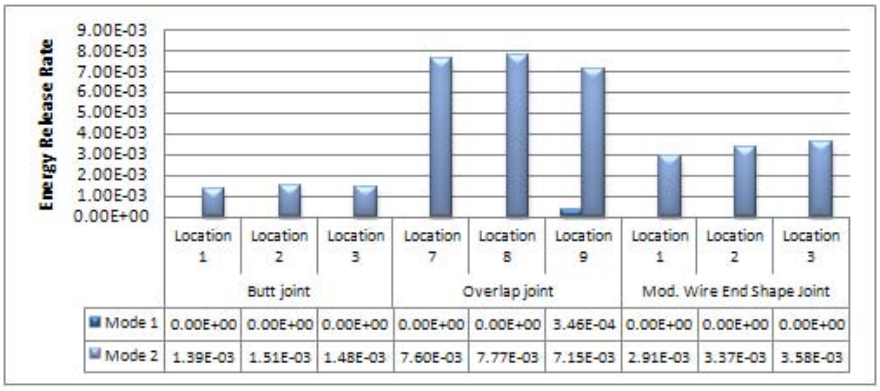

Figure 17. Energy Release Rate of Resin Cracks between the Fibers for Each Joint Design.

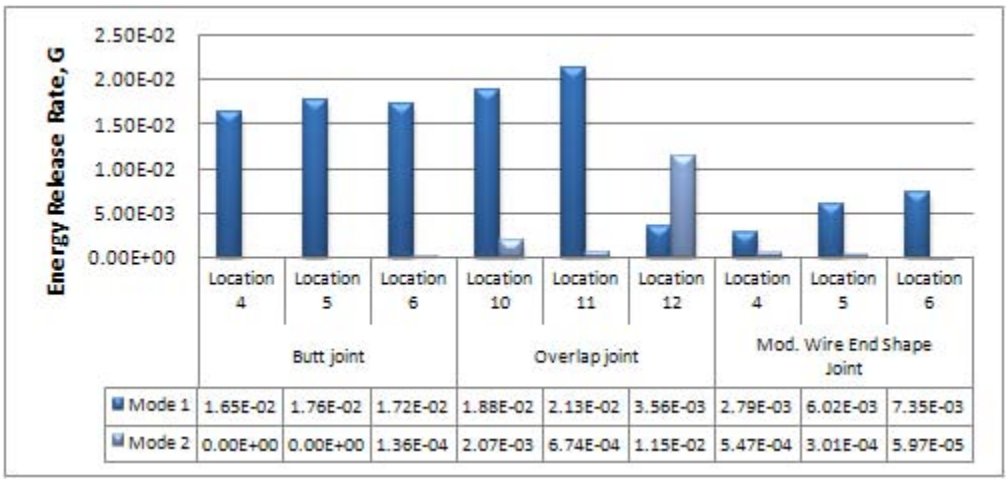

Figure 18. Most Critical Energy Release Rate of Resin Cracks between the Fibers Tips for each Joint.

Based on these results, in cases where high stresses exist between the fibers, the butt joint is the best design to be considered. And in cases where high stresses exist in between the fiber tips, the modified-wire-end-shape joint is proposed. For the overlap joint, this design can be considered under small tension loading.

C. INFLUENCE OF WIRE END GEOMETRY AND MIDDLE LAYER GAP

Further investigation was made to determine the influence of the resin area between the fiber tips and the wire end geometry: between the butt joint and modified-wire-end-shape joint. This was done by applying a tensile load to the models and extending the gap d between the middle layers, as shown in Figure 19, to the point where the middle fiber tips has no significant interaction; and thus will have no effect on the energy release rate of an existing crack place between the metal wire and e-glass fiber. The numerical results revealed that tip geometry has minimal effect on the energy release rate of the crack at a very wide gap.

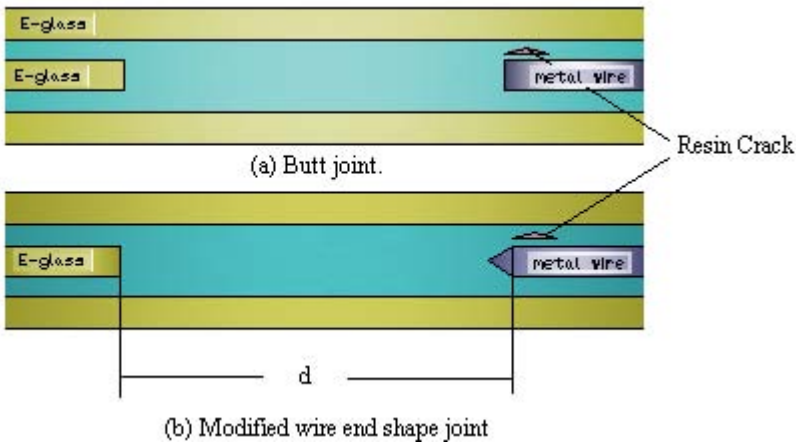

Figure 19. Butt Joint and Modified-Wire-End-Shape joint with Middle Gap Extended.

Another analysis made was extending the gap d incrementally and comparing the shear stress in the resin between the fibers near the discontinuity. The results showed that as the resin area in between the fiber tips was increased, the shear stresses between the fibers near the discontinuity also increased. This means that with greater resin area between the fiber tips, the resin deforms more freely, thereby shifting some of the load to the resin between the fibers near the discontinuity; carried in the form of shear stress.

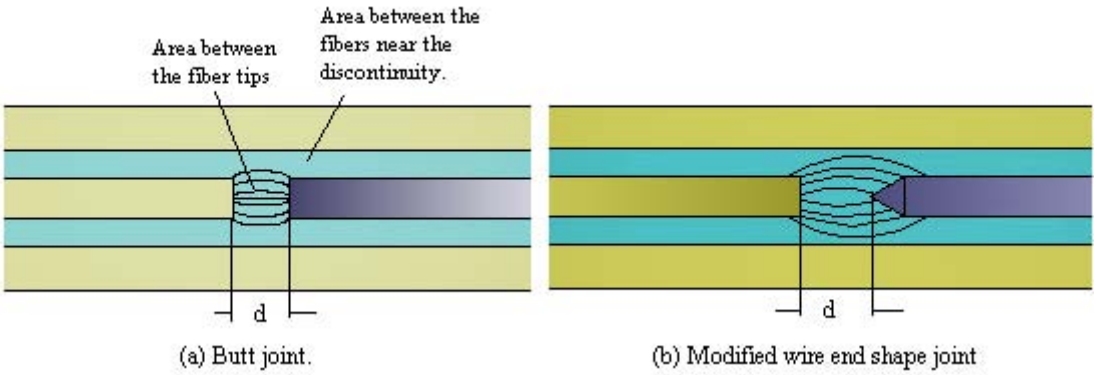

Figure 20. Middle Fiber Interaction of the Butt Joint and Modified-Wire-End-Shape Joint.

Figure 20 shows the strain between the tips represented by the field lines, for the same gap d. In the case of the butt joint there is a very small area filled by the resin, the

strain fields are more concentrated at the tip edges, thereby having less influence on the crack Locations 1 through 3 (Figure 11), while having greater influence for the cracks in Locations 4 through 6 (Figure 12). In the case of the modified-wire-end-shape joint, which have a larger resin area between the tips, the strain fields are not as concentrated compared to the butt joint. This allows the resin between the tips to deform more freely, which influences the cracks in Locations 1 through 3 in Figure 15 and less influence on the crack Locations 4 through 6 in Figure 16 by shifting some of the load to the resin between the fiber tips near the discontinuity. Figures 21 and 22 shows the comparison of the butt joint and modified-wire-end-shape joint.

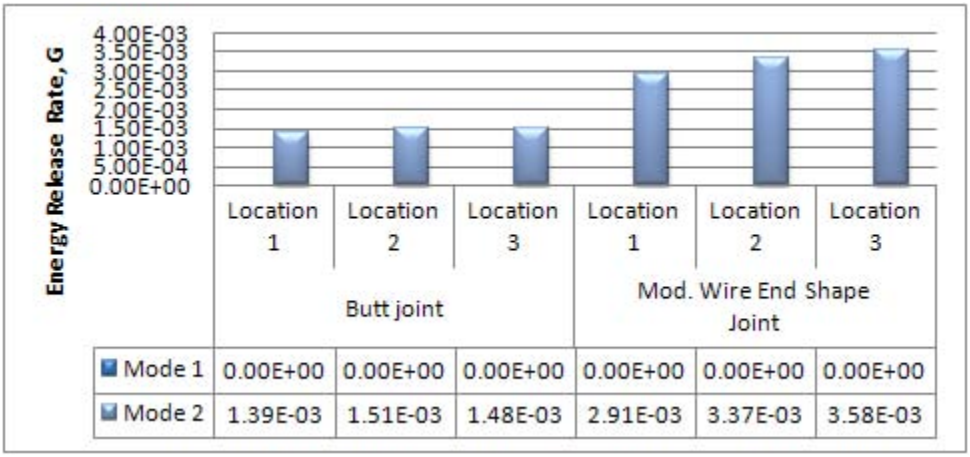

Figure 21. Comparison of the Resin Cracks between the Fibers for the Butt Joint and Modified-Wire-End-Shape Joint.

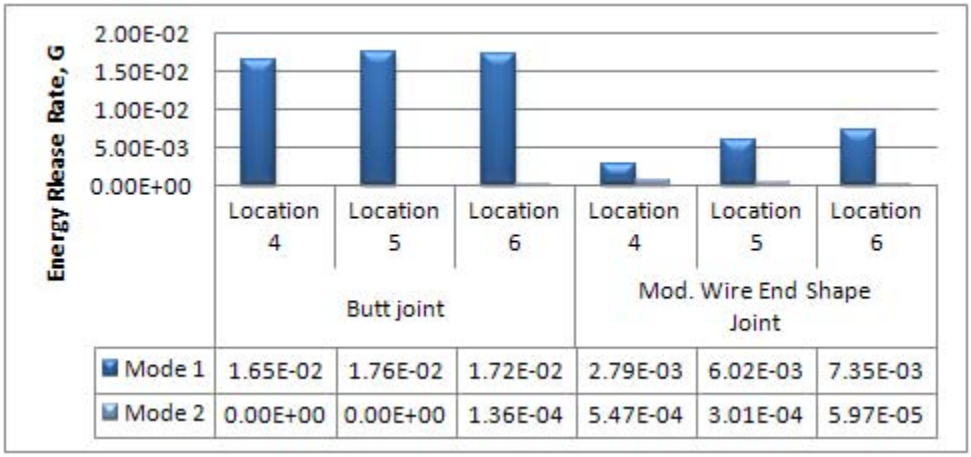

Figure 22. Comparison of the Resin Cracks between the Tips of the Fibers for the Butt Joint and Modified-Wire-End-Shape Joint.

For the overlap joint, varying the overlap angle changes the area filled by the resin between the inclined edge and the metal wire tip as shown in Figure 23. This influences the energy release rate of the cracks in the same way.

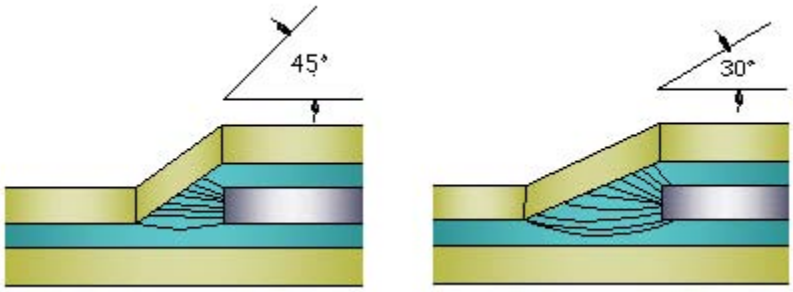

Figure 23. Metal Wire Tip and Inclined edge Interaction of the Overlap Joint.

THIS PAGE INTENTIONALLY LEFT BLANK

IV. ANALYSIS AND RESULTS FOR LOADING IN SHEAR

A. RESULTS AND DISCUSSION

1. Critical Locations

The resulting effective mechanical strain plots of the models, without defects, under shear in the –y direction are shown in Figure 24 through 26. The regions of high strain for the butt joint are located around the left edge corners of the metal wire mat. Although opposite in direction, the magnitude of the upper and lower strain fields are equal; thus the upper half (Figure 24) of the model was considered for the analysis. For the overlap joint, three critical crack locations were considered since the resulting plot (Figure 25) shows three regions of high strain. In the case of the modified-wire-end-shape joint, the regions of high strain are located at the corners of the wire tip (Figure 26). The upper half of the model was considered for the analysis, since the strain fields are equal in magnitude, although opposite in direction.

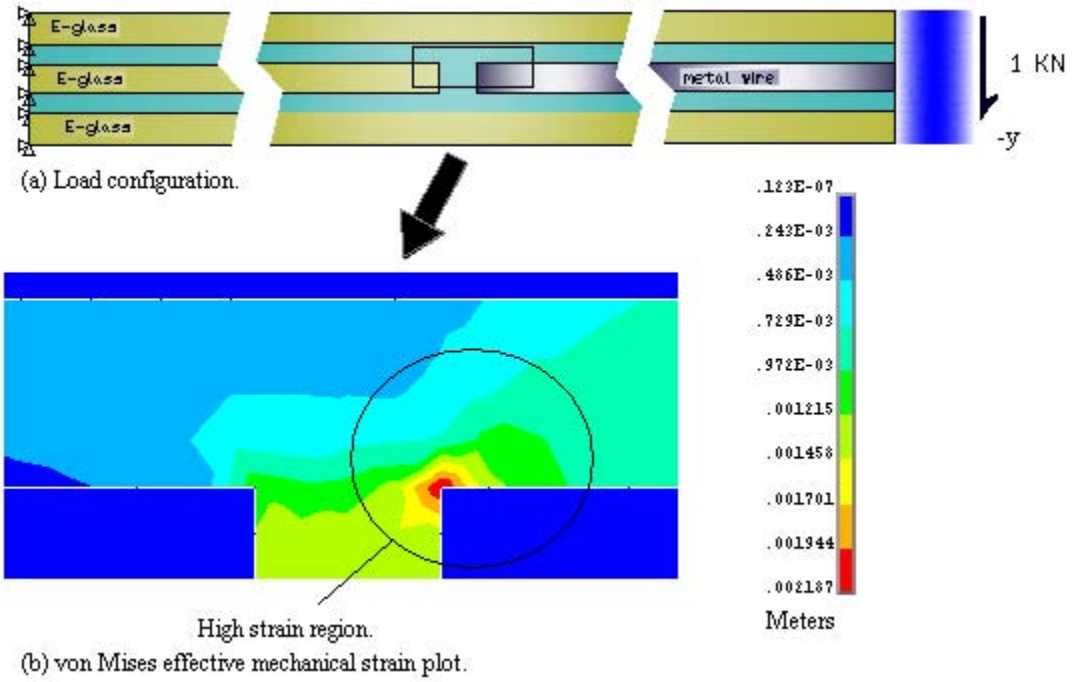

Figure 24. Butt Joint Critical Location.

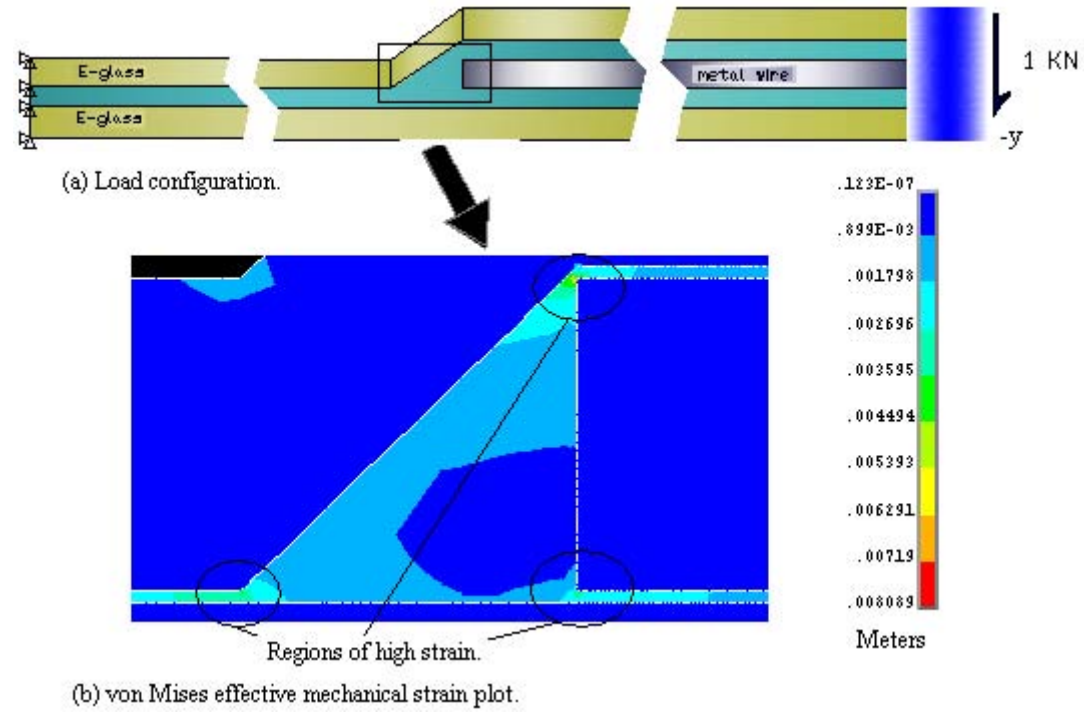

Figure 25. Overlap Joint Critical Location

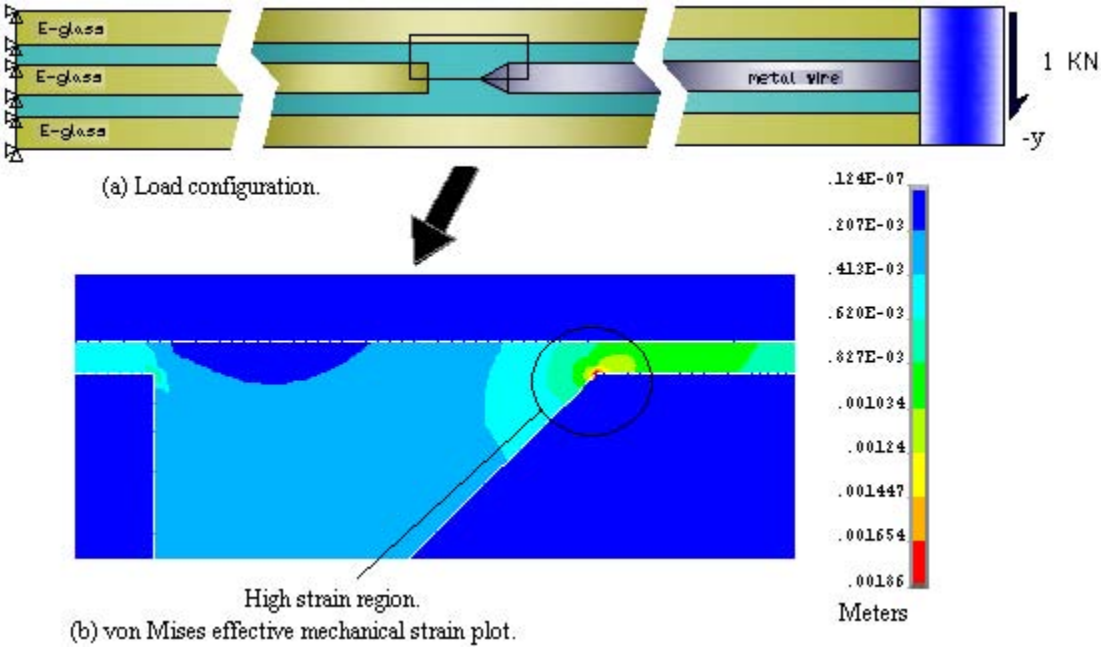

Figure 26. Modified-Wire-End-Shape Joint Critical Location

For this load case, shear loading in the +y direction was also investigated to determine the tensile and compressive effects on the crack locations that were previously

analyzed. The onset of crack growth in the resin may occur between the fibers or between the middle fiber tips. In this analysis, particular attention was given separately to the resin cracks between the fibers and between the middle fiber tips.

2. Energy Release Rate Results

a. Butt Joint

In Location 1 through 3 in Figure 27, it was observed that the forces acting on the crack are closing in nature. With the upper half under tension, the mode I energy release rate component is non-existent and the energy release rate is purely mode II for resin cracks located between the fibers. The energy release rate results shows that the crack inside the resin, Location 2 in Figure 27, is the most critical case.

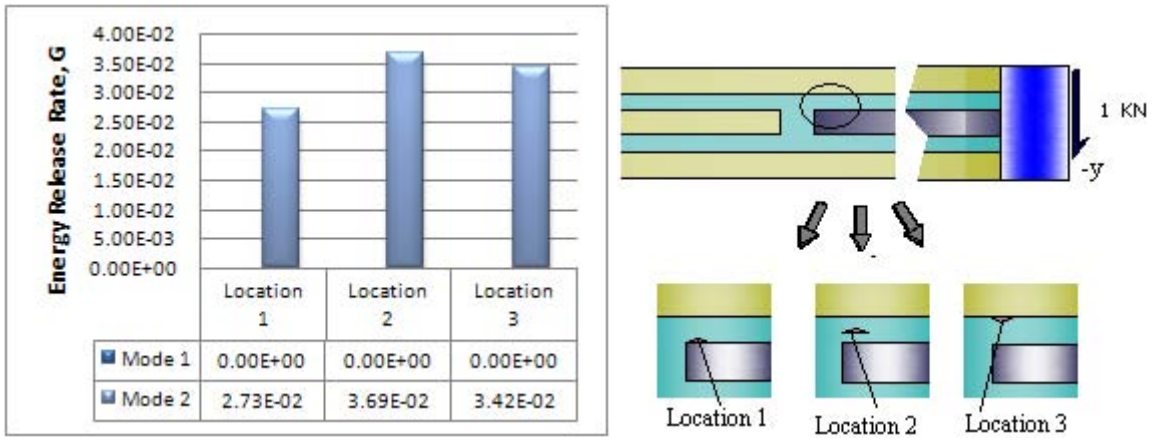

Figure 27. Butt Joint: Energy Release Rate of Resin Cracks between the Fibers (Shear Loading in the –y direction).

With the shear load reversed, now in the +y direction, Figure 28 shows the existence of mode I and II. This means that the forces acting on the crack are opening in nature when the upper part of the model is under compression. Results yield the same mode II values, except in this case mode I components are present.

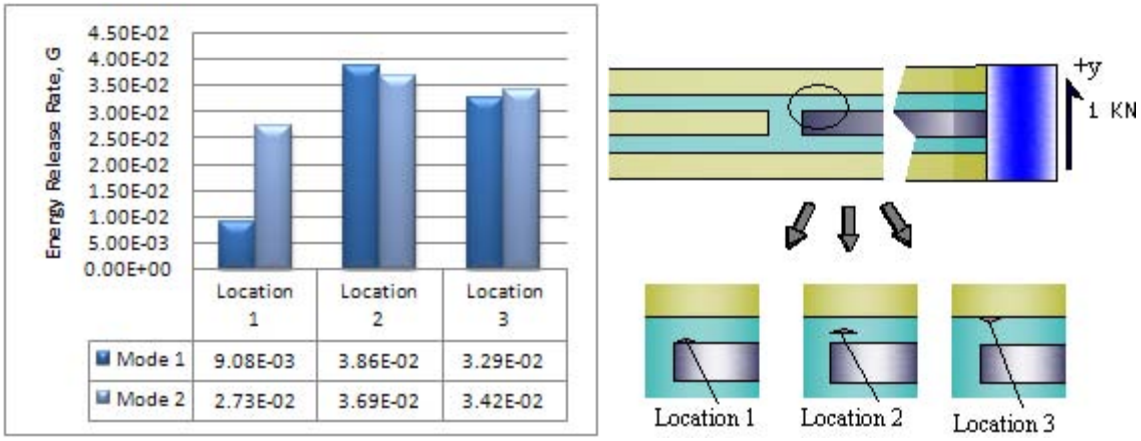

Figure 28. Butt Joint: Energy Release Rate of Resin Cracks between the Fibers (Shear Loading in the +y direction).

Figure 29 shows the results for shear loading in the –y direction. Shear loading in the +y directions revealed similar mode II results; however, mode I components are non-existent due to forces are closing in nature. Although there is no significant difference between the energy release rate results of Location 4 through 6, Location 5, which is the crack inside the resin, is the most critical case.

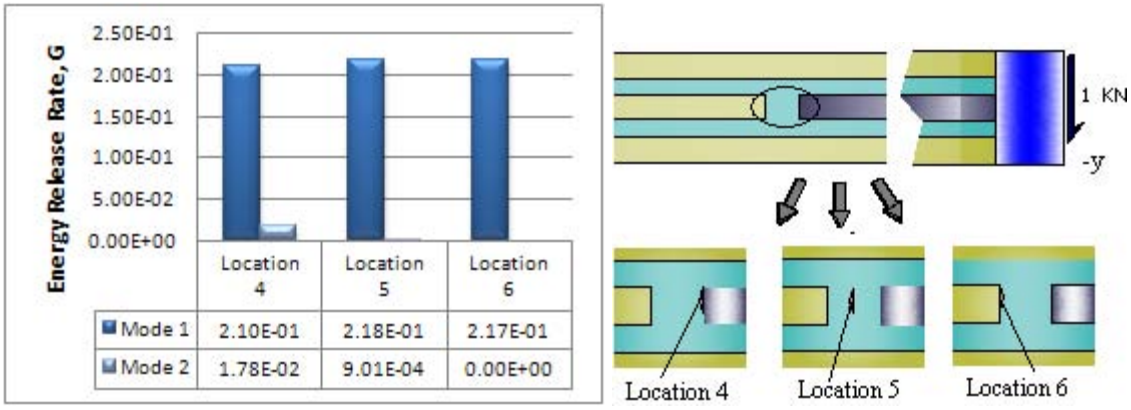

Figure 29. Butt Joint: Energy Release Rate of Resin Cracks between the Fibers Tips (Shear Loading in the -y direction).

b. Overlap Joint

Figure 30a, shear load in the –y direction, shows that Location 8 is the most critical case; while in Figure 30c, shear load in +y direction, shows that Location 2 is the most critical case. Since Location 2 in Figure 30c have a higher mode I energy release rate results, which is more critical than mode II; Location 2 under shear loading in the +y direction was considered to be the most critical case.

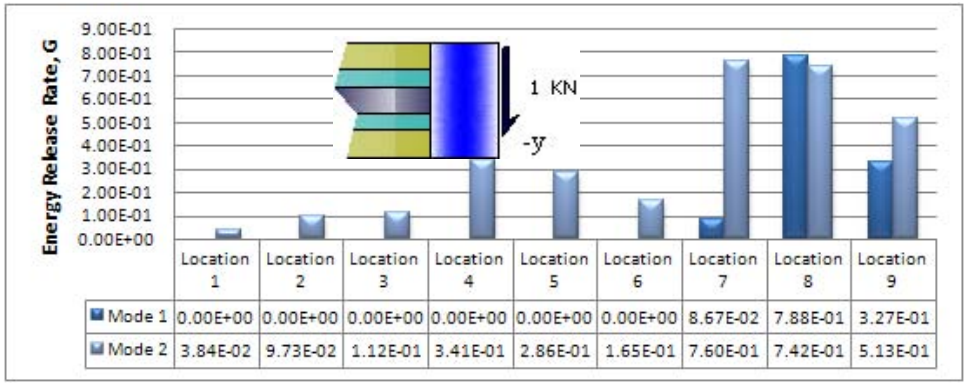

	Location 1	Location 2	Location 3	Location 4	Location 5	Location 6	Location 7	Location 8	Location 9
Mode 1	0.00E+00	0.00E+00	0.00E+00	0.00E+00	0.00E+00	0.00E+00	8.67E-02	7.88E-01	3.27E-01
Mode 2	3.84E-02	9.73E-02	1.12E-01	3.41E-01	2.86E-01	1.65E-01	7.60E-01	7.42E-01	5.13E-01

(a) –y shear load.

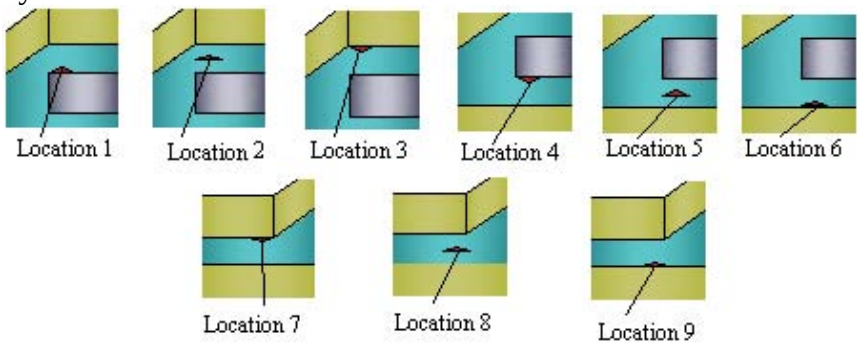

(b) Crack Locations.

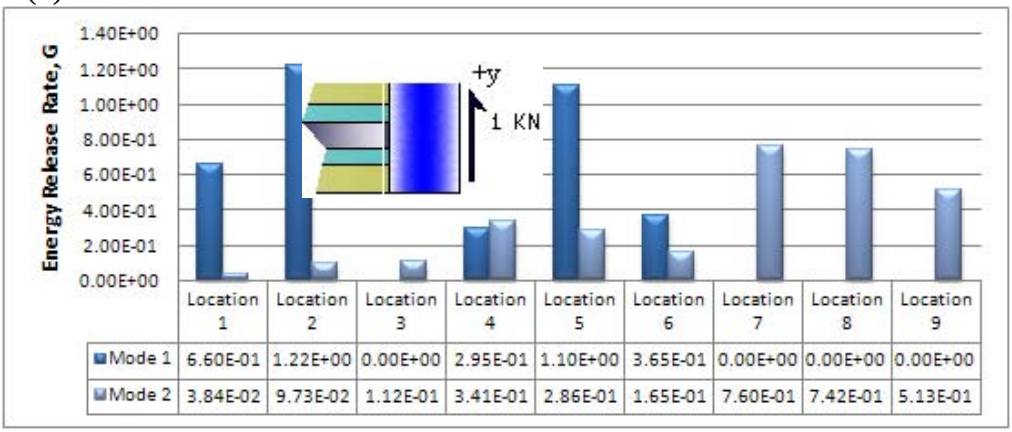

	Location 1	Location 2	Location 3	Location 4	Location 5	Location 6	Location 7	Location 8	Location 9
Mode 1	6.60E-01	1.22E+00	0.00E+00	2.95E-01	1.10E+00	3.65E-01	0.00E+00	0.00E+00	0.00E+00
Mode 2	3.84E-02	9.73E-02	1.12E-01	3.41E-01	2.86E-01	1.65E-01	7.60E-01	7.42E-01	5.13E-01

(c) +y shear loading.

Figure 30. Overlap Joint: Energy Release Rate of Resin Cracks between the Fibers.

Figure 31 shows the results for shear loading in the –y direction. Shear loading in the + y direction yield the same mode II results except that the mode I components are non-existent. Results show that Location 12 is the most critical case.

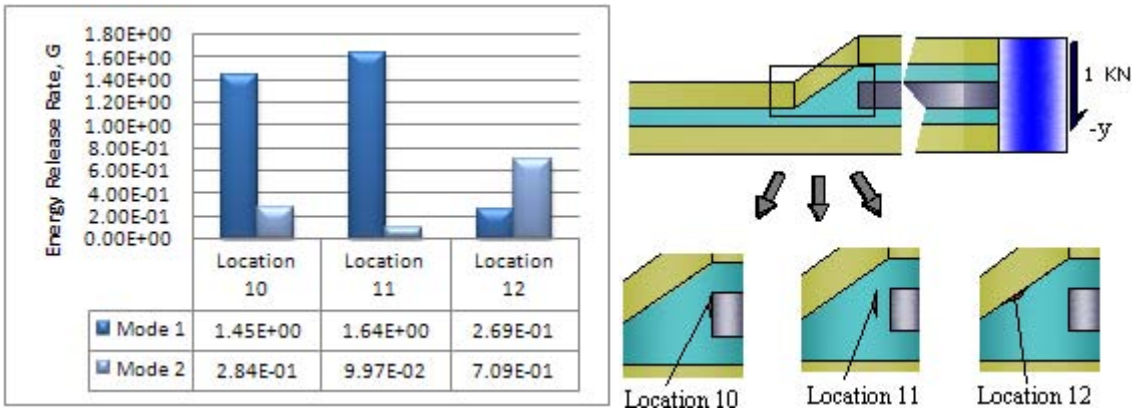

Figure 31. Overlap Joint: Energy Release Rate of Resin Cracks between the Fibers.

c. Modified-Wire-End-Shape Joint

In Location 1 through 3 in Figure 32, it was observed that the forces acting on the crack are closing in nature. With the upper half under tension, the mode I energy release rate component is non-existent and the energy release rate is purely mode II for resin cracks located between the fibers. The energy release rate results shows that the crack inside the resin, Location 2 in Figure 32, is the most critical case.

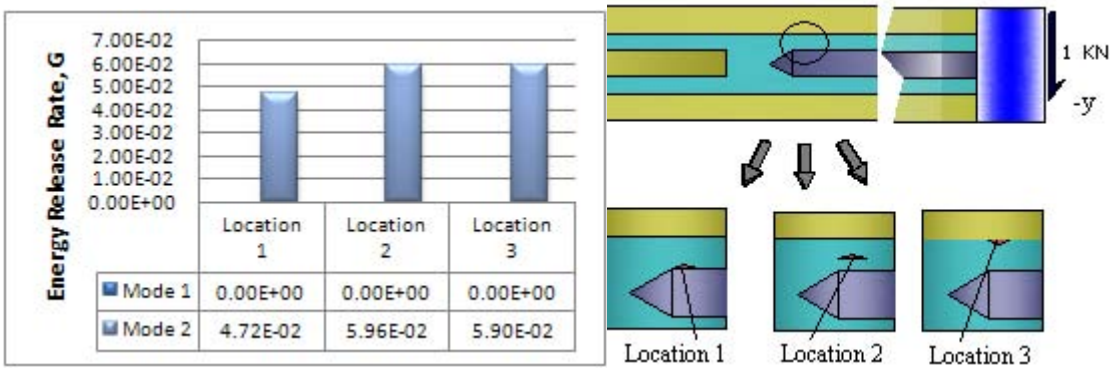

Figure 32. Modified-Wire-End-Shape Joint: Energy Release Rate of Resin Cracks between the Fibers (Shear Loading in the –y direction).

With the shear load reversed, +y direction, Figure 33 shows the existence of mode I and II. This means that the forces acting on the crack are opening in nature when the upper part of the model is under compression. Results yield the same mode II values, except in this case mode I components are present.

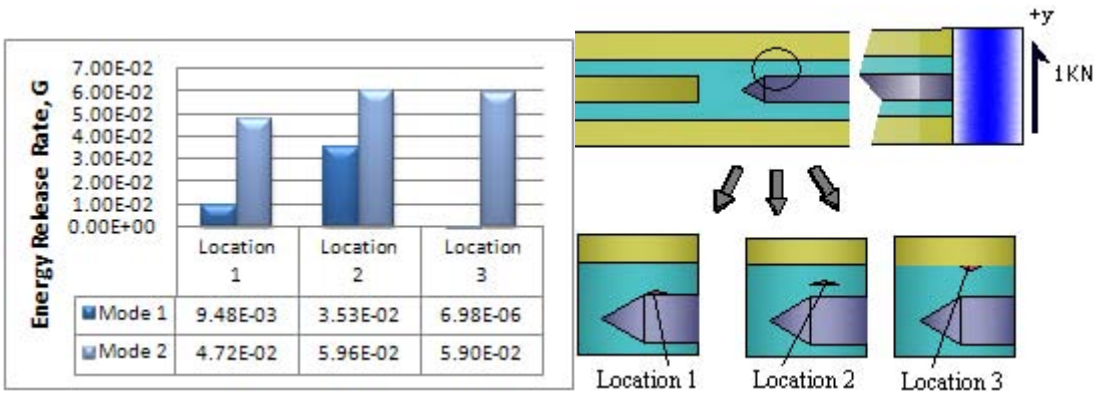

Figure 33. Modified-Wire-End-Shape Joint: Energy Release Rate of Resin Cracks between the Fibers (Shear Loading in the +y direction).

B. SUMMARY

Figure 34 (shear load in the +y direction) and Figure 35 (shear load in the –y direction) shows the comparison of the energy release rate for each joint design. It was observed that the overlap joint has the highest energy release rate results for resin cracks between the fibers and in between the fiber tips. For resin cracks between the fibers, the butt joint gave lower energy release rate results than the modified-wire-end-shape joint. However, for the resin cracks between the fiber tips the modified-wire-end-shape joint gave lower results. For the crack locations investigated the most critical case for each joint are the cracks inside the resin.

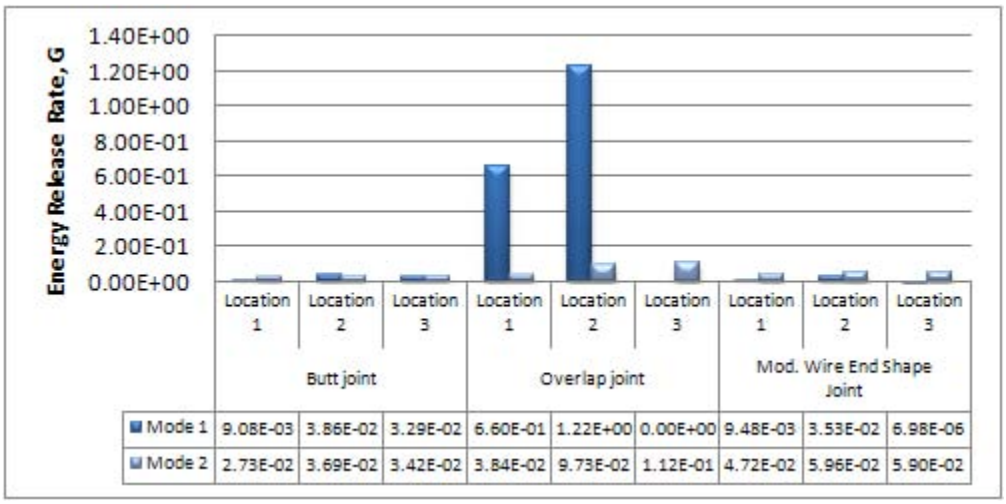

Figure 34. Energy Release Rate of Resin Crack between the Fibers for each Joint.

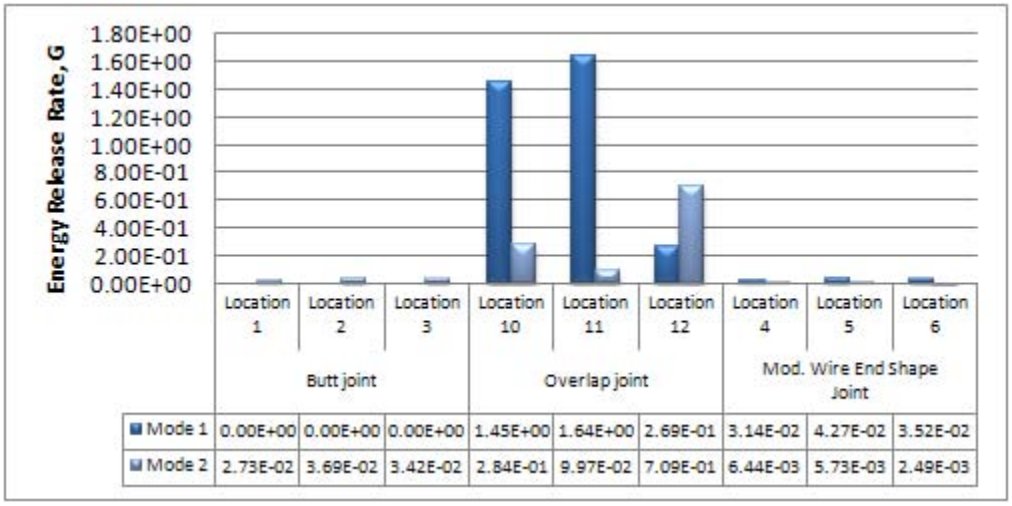

Figure 35. Release Rate of Resin Crack between the Fiber Tips for each Joint.

Based on these results, in cases where high stresses exist between the fibers, the butt joint is the best design to be considered. In cases where high stresses exist in between the fiber tips, the modified-wire-end-shape joint is proposed. For the overlap joint, this design can be considered under small shear loading.

V. ANALYSIS AND RESULTS FOR BENDING LOAD

A. RESULTS AND DISCUSSION

1. Critical Locations

The resulting effective mechanical strain plots of the models, without defects, under clockwise (CW) bending are shown in Figure 36 through 38. The regions of high strain for the butt joint are located around the left edge corners of the metal wire mat. Although opposite in direction, the upper and lower strain fields are equal in magnitude, the upper half (Figure 36) of the model was considered for the analysis. For the overlap joint, three critical crack locations were considered since the resulting strain plot (Figure 37) shows three regions of high strain. In the case of the modified-wire-end-shape joint, the regions of high strain are located at the corners of the wire tip (Figure 38). The upper half of the model was considered for the analysis, since the strain fields are symmetrical about its centerline, although opposite in direction.

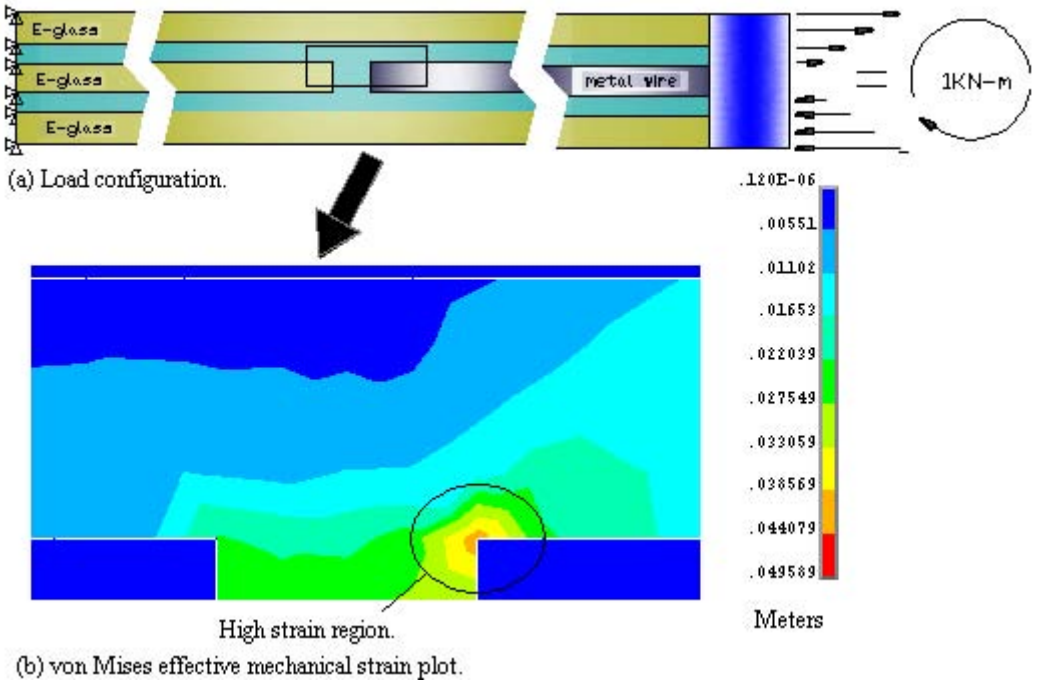

Figure 36. Butt Joint Critical Location.

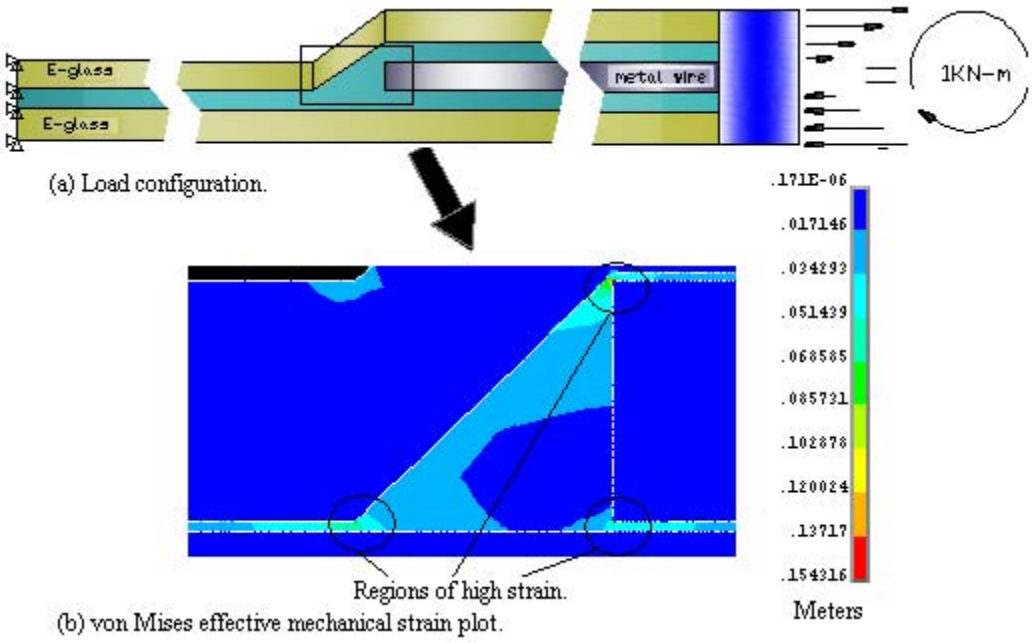

Figure 37. Overlap Joint Critical Location.

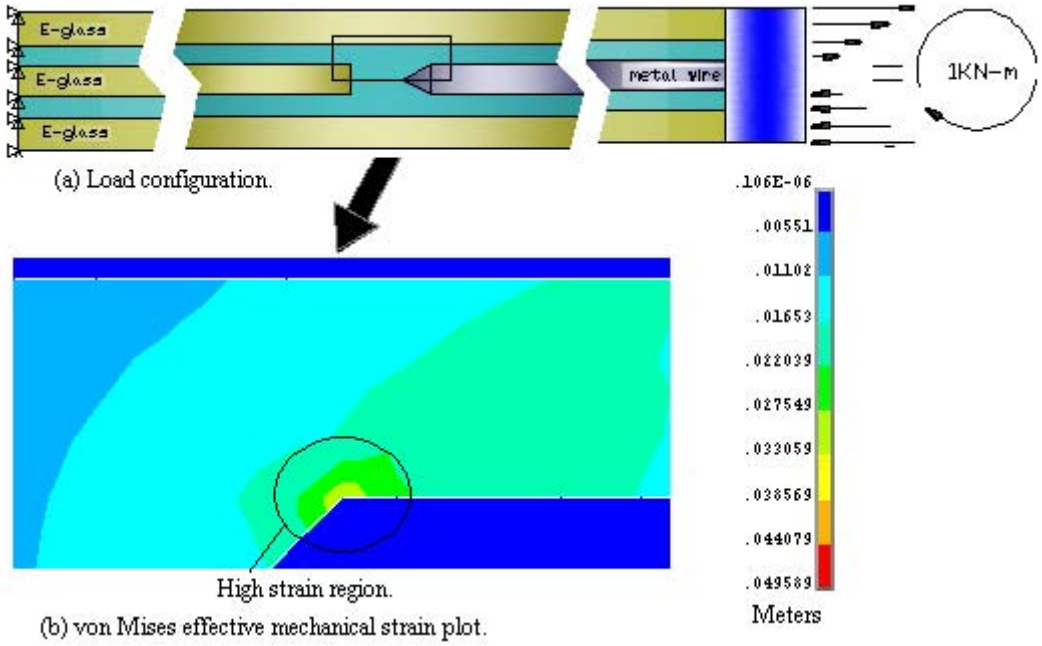

Figure 38. Modified-Wire-End-Shape Joint Critical Location.

For this load case, clockwise (CW) and counter clockwise (CCW) bending were investigated to determine the tensile and compressive effects on the crack locations that

were previously analyzed. The onset of crack growth in the resin may occur between the fibers or between the middle fiber tips. Once again in this analysis, particular attention was given separately to the resin cracks between the fibers and between the middle fiber tips.

2. Energy Release Rate Results

a. Butt Joint

CCW bending was considered for the analysis since mode I component for CW loading is non-existent. Figure 39 shows Location 2, which is the crack inside the resin, to be the most critical case.

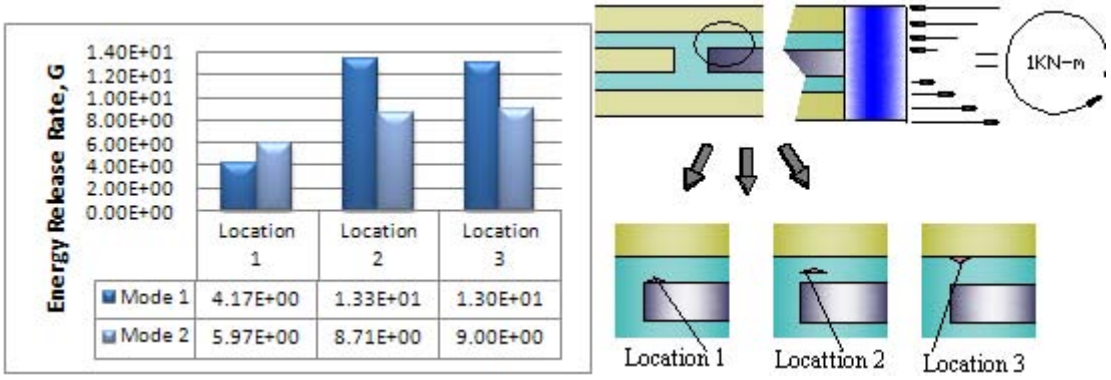

Figure 39. Butt Joint: Energy Release Rate of Resin Cracks between the Fibers (CCW Bending).

In Figure 40, although there is no significant difference between the energy release rate results of Location 4 through 6; Location 5, which is slightly highest, is the most critical case.

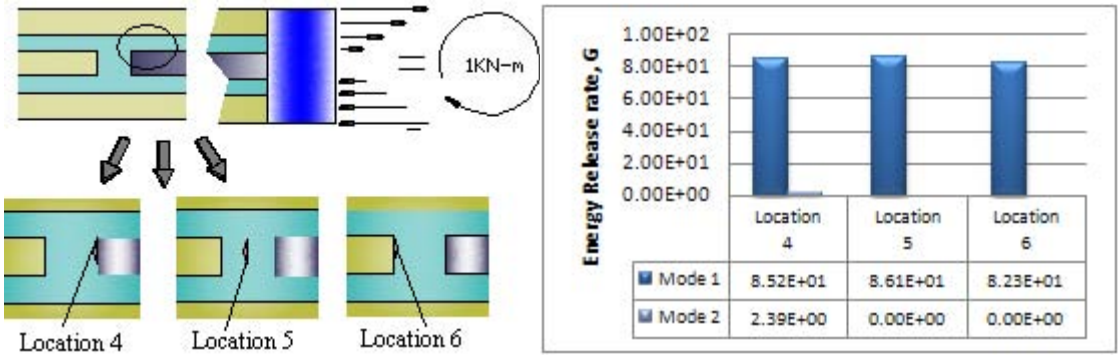

Figure 40. Butt Joint: Energy Release Rate of Resin Cracks between the Fibers Tips (CW Bending).

b. Overlap Joint

Figure 41a, with CW bending, shows that Location 8 is the most critical; while in Figure 41c, CCW bending, shows that Location 5 is the most critical case. Since Location 5 in Figure 41c have a higher mixed mode energy release rate results, Location 5 under CCW bending was considered to be the most critical crack case.

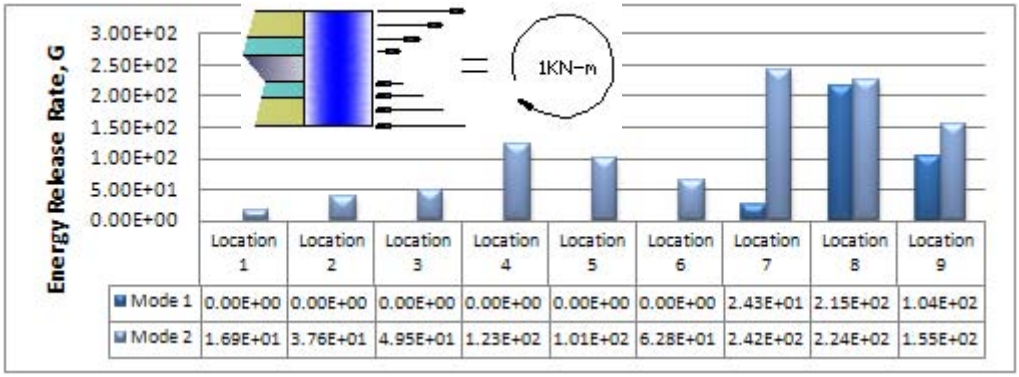

(a) CW bending.

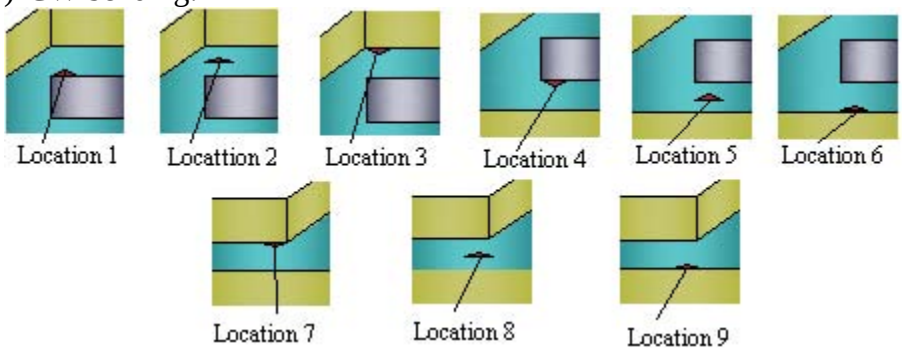

(b) Crack Locations.

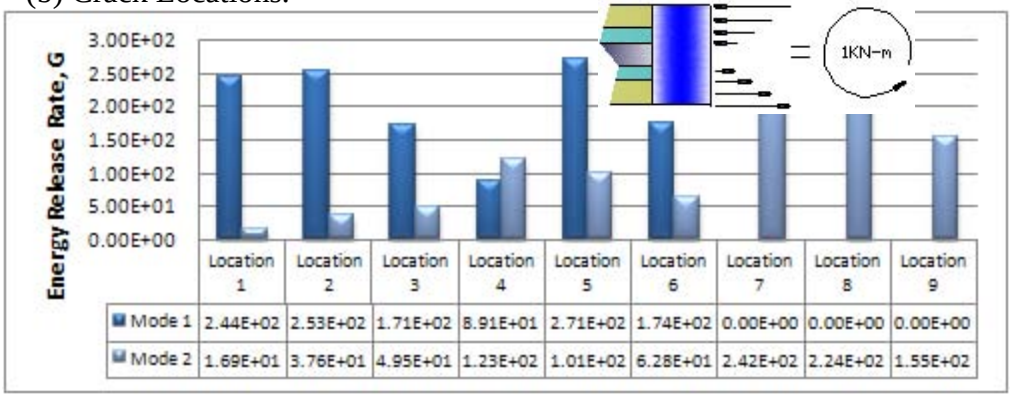

(c) CCW bending.

Figure 41. Overlap Joint: Energy Release Rate of Resin Cracks between the Fibers.

Figure 42 show the results for CW bending. Results show that Location 11 is the most critical case.

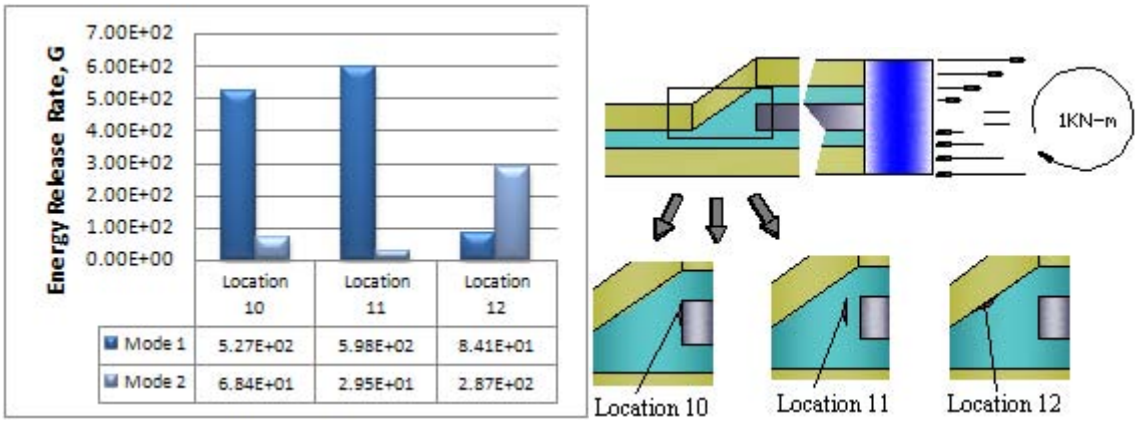

Figure 42. Overlap Joint: Energy Release Rate of Resin Cracks between the Fibers.

c. Modified-Wire-End-Shape Joint

Under CW bending mode I and II components are present while in CCW bending mode I are non-existent due to the closing nature of the forces acting on the crack locations shown in Figure 43. The energy release rate results of the cracks between the fibers shows that the crack inside the resin, Location 2 in Figure 43, is the most critical case.

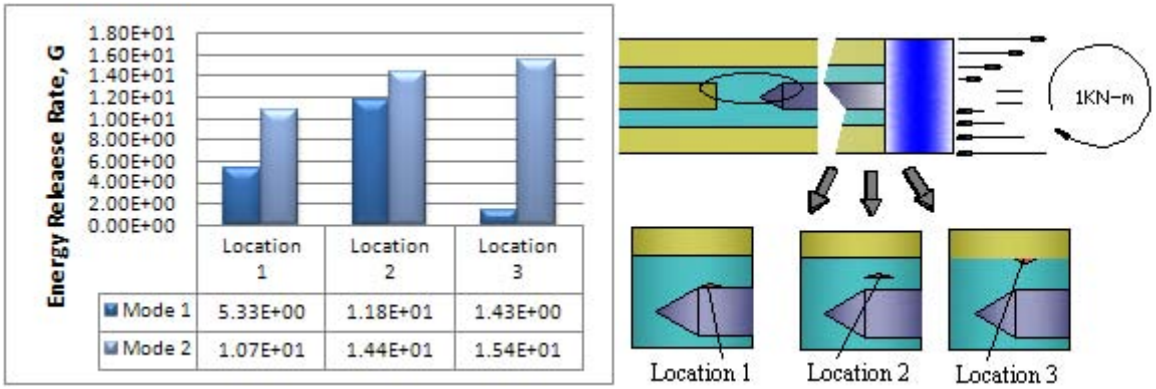

Figure 43. Modified-Wire-End-Shape Joint: Energy Release Rate of Resin Cracks between the Fibers (CW Bending).

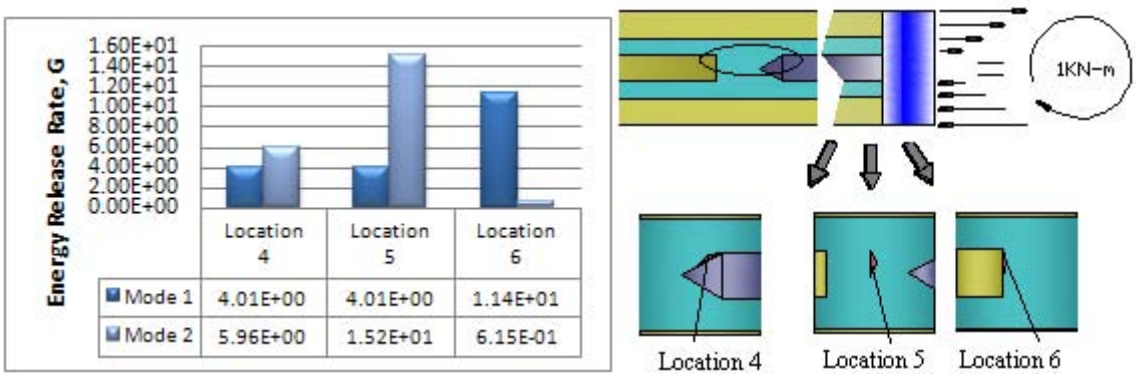

Figure 44. Modified-Wire-End-Shape Joint: Energy Release Rate of Resin Cracks between the Fibers (CW Bending).

B. SUMMARY

Figure 45 (CCW bending) and Figure 46 (CW bending) shows the comparison of the energy release rate for each joint design. It was observed that the overlap joint has the highest energy release rate results for resin cracks between the fibers and in between the fiber tips. For resin cracks between the fibers, the butt joint gave lower energy release rate results than the modified-wire-end-shape joint. However, for the resin cracks between the fiber tips, the modified-wire-end-shape joint gave lower results. In all the crack locations investigated the most critical case for each joint are the cracks inside the resin.

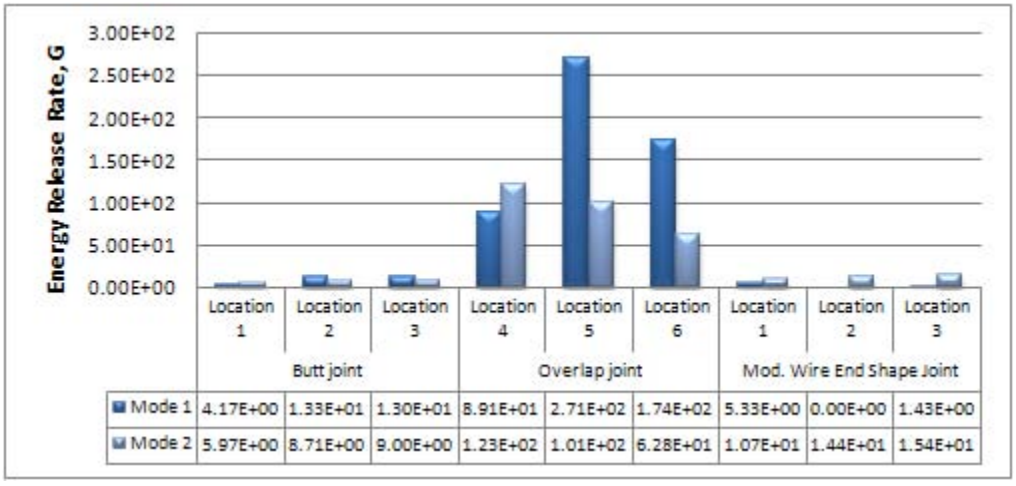

Figure 45. Energy Release Rate of Resin Cracks between the Fibers for Each Joint.

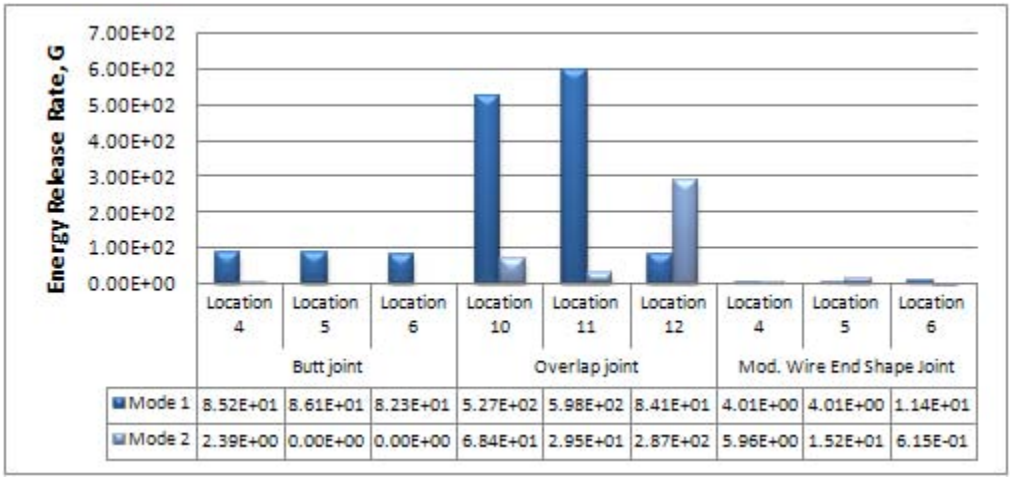

Figure 46. Energy Release Rate of Resin Cracks between the Fiber Tips for each Joint.

Based on these results, in cases where high stresses exist between the fibers, the butt joint is the best design to be considered. In cases where high stresses exist in between the fiber tips, the modified-wire-end-shape joint is proposed. For the overlap joint, this design can be considered under small bending loads.

THIS PAGE INTENTIONALLY LEFT BLANK

VI. CONCLUSION AND RECOMMENDATION

In all the load cases that were investigated, the butt joint proved to be the best joint to be considered in situations where the stresses at the butted ends are relatively low; while the modified-wire-end-shape proved to be the joint to be considered in situations where the stresses between the fiber tips are high. An example where these situations apply is the symmetric stepped-lap joint under tension shown in Figure 47. Previous numerical analysis of this type of joint showed that the resin between the butted ends of the center ply carries higher stresses than the resin between the butted ends of the outer plies.

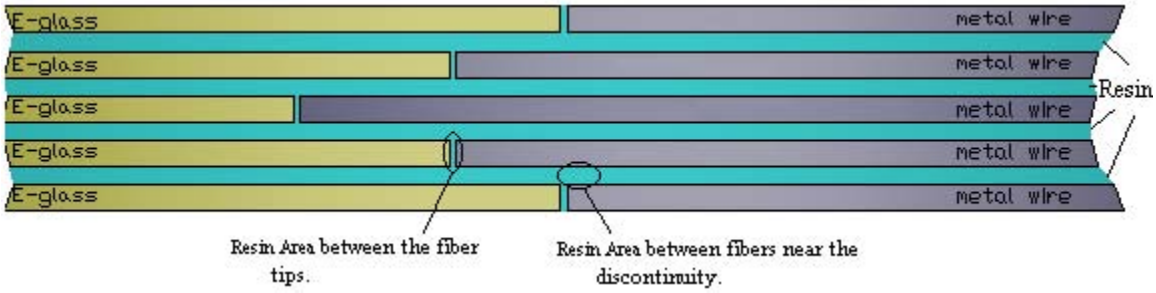

Figure 47. Symmetric Stepped-Lap Joint.

From what has been determined in this research, one way of improving the joint in terms of fracture toughness is to increase the gap between the butted ends of the center ply. Performing this step increases the resin area between the tips which allows the resin to deform more freely thus shifting the load. The load that is shifted is carried by shear stress developed in the resin between the fibers near the discontinuity. However, increasing the gap can require careful spacing of the fibers and can be time consuming in the manufacturing process. An alternative is to modify the wire end. This step increases the resin area between the fiber tips and it can eliminate the time spent in spacing the fibers since it can easily be pushed together with the e-glass fiber mat. Figure 48 show a proposed joint configuration for the symmetric stepped-lap Joint.

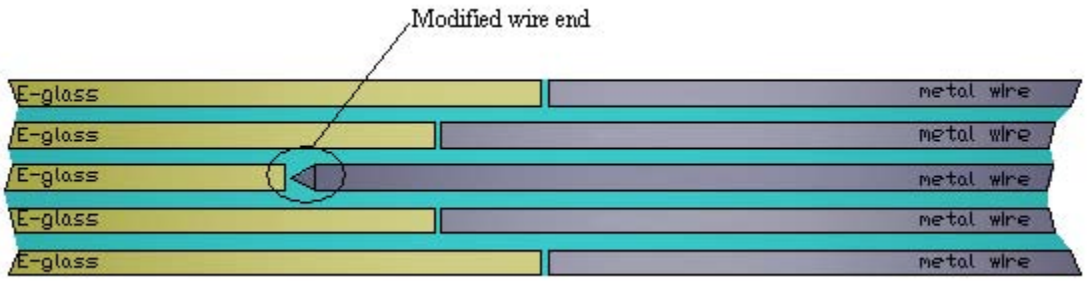

Figure 48. Design Modification for Symmetric Stepped-Lap Joint.

In the case of the overlap joint, it showed poor results relative to the other two joints analyzed. Although it is the best choice in terms of lesser material used in manufacturing, the overlap joint can be considered provided that the load is not large enough to exceed the critical fracture toughness.

To determine the significance of altering the wire end, testing and numerical modeling is recommended for future work in comparing butted joints and where the modified-wire-end-shape joint is incorporated.

LIST OF REFERENCES

[1] J. Reddy and A. Miravite, "Practical Analysis of Composite Laminates," CRC Press, Inc., Florida, 1995.

[2] R. Krueger, "The Vitual Crack Closure Technique: History, Approach and Applications," NASA/CR-211628, 2002.

[3] W. Schultz, "Experimental Study of Composite and Metal-Wire Joints," M.S. Thesis, Naval Postgraduate School, Monterey, California, 2008.

[4] T. Greene, T, "Analytical Modeling of Composite-to-Composite (SCARF) Joints in Tension and Compression," M.S. Thesis, Naval Postgraduate School, Monterey, California, 2007.

[5] R. Krueger, "A Method for Calculating Strain Energy Release Rate in Preliminary Design of Composite Skin/Stringer Debonding Under Multi-axial Loading," NASA/TM-209365, 1999.

[6] M. Crane, T. Robbins and S. Graham, "Influence of Joint Geometry on Tensile Strength of a Co-Cured Symmetric Stepped-Lap Joint," presented at SAMPE-2005 Conference, May1-5, Long Beach, California, 2005.

THIS PAGE INTENTIONALLY LEFT BLANK

INITIAL DISTRIBUTION LIST

1. Defense Technical Information Center
   Ft. Belvoir, Virginia

2. Dudley Knox Library
   Naval Postgraduate School
   Monterey, California

3. Professor Young Kwon
   Naval Postgraduate School
   Monterey, California

4. Douglas C. Loup
   Naval Surface Warfare Center, Carderock Division
   West Bethesda, Maryland

5. Erik A. Rasmussen
   Naval Surface Warfare Center Carderock Division
   West Bethesda, Maryland

6. Scott W. Bartlett
   Naval Surface Warfare Center Carderock Division
   West Bethesda, Maryland

7. Engineering and Technology Circular Office, Code 34
   Naval Postgraduate School
   Monterey, California